SUPPLEMENT 6

HONG KONG MEDICAL JOURNAL 香港醫學雜誌 Volume 20 Number 6 December 2014 Supplement 6

HONG KONG Volume 20 Number 6 December 2014

The official publication of the
Hong Kong Academy of Medicine and
the Hong Kong Medical Association

MEDICAL JOURNAL
香港醫學雜誌

Research Fund for the Control of Infectious Diseases

Research Dissemination Reports

控制傳染病研究基金

研究成果報告

Influenza
流感

Viral hepatitis
病毒性肝炎

Human papillomavirus
人類乳頭瘤狀病毒

ISSN 1024-2708

香港醫學專科學院出版社
HONG KONG ACADEMY OF MEDICINE PRESS

HONG KONG MEDICAL JOURNAL 香港醫學雜誌
Volume 20 Number 6 **December 2014**
SUPPLEMENT 6

Research Fund for the Control of Infectious Diseases

Research Dissemination Reports

INFLUENZA

VIRAL HEPATITIS

HUMAN PAPILLOMAVIRUS

Editorial

Dissemination reports are concise informative reports of health-related research supported by funds administered by the Food and Health Bureau, for example the *Research Fund for the Control of Infectious Diseases* (which was consolidated into the Health and Medical Research Fund in December 2011). In this edition, 12 dissemination reports of projects related to influenza, viral hepatitis, and human papillomavirus are presented. In particular, three projects are highlighted due to their potentially significant findings, impact on healthcare delivery and practice, and/or contribution to health policy formulation in Hong Kong.

Innate and adaptive immune systems play critical roles in protecting against infection. Tu et al[1] aimed to develop alternative strategies to activate early innate responses—the host's first line of defence—against influenza A virus infection. Using a mouse model with a human immune system, they demonstrated that phosphoantigen could protect against influenza A H1N1 virus infection. For avian influenza A H5N1 virus infections, this protection was strain-dependent. This study suggested a potentially novel therapeutic approach for influenza using phosphoantigens to inhibit influenza infection.

Chronic hepatitis B (CHB) is the most common cause of liver cirrhosis and hepatocellular carcinoma in most Asian countries. Chan et al[2] validated the performance of an ALT-based transient elastography algorithm and various serum test formulae in a cohort of 82 newly-recruited ethnic Chinese CHB patients. They developed an algorithm to predict advanced liver fibrosis in CHB. This algorithm improved the accuracy of prediction compared with transient elastography alone, and liver biopsy could be correctly avoided in approximately 50% of patients.

Human papillomavirus (HPV) is a common sexually transmitted pathogen that plays an important role in the pathogenesis of pre-cancerous cervical lesion and cervical cancer. Integration of HPV genetic material into the host genome correlates with poor response to treatment and poor disease-free survival in cervical cancer. Liu et al[3] studied the spectrum and prevalence of HPV in healthy women in Guangzhou and Hong Kong and determined the extent and clinical significance of integration of HPV16 and HPV58 genomes in the host in relation to precancerous lesion and cervical cancer. They found that women in Guangzhou had significantly higher HPV prevalence than those in Hong Kong. Younger women had significantly higher risk of HPV infection.

A research impact evaluation was conducted 2 years after the project end date for all studies reported in this supplement. Many of the studies reported impact through knowledge generation, capacity building, and influence on health policy and health care practices.

We hope you will enjoy this selection of research dissemination reports. Electronic copies of these dissemination reports and the corresponding full reports can be downloaded individually from the Research Fund Secretariat website (http://www.fhb.gov.hk/grants). Researchers interested in the funds administered by the Food and Health Bureau also may visit the website for detailed information about application procedures.

Supplement co-editors

Dr Ivy Cheung
Chief Secretariat Executive
(Research Office)
Food and Health Bureau

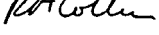

Dr Richard A. Collins
Scientific Review Director
(Research Office)
Food and Health Bureau

References

1. Tu WW, Lau YL, Peiris JS. Use of humanised mice to study antiviral activity of human γδ-T cells against influenza A viruses. Hong Kong Med J 2014;20(Suppl 5):4-6.
2. Chan HL, Wong VW, Wong GL, Choi PC. Non-invasive algorithm for detecting advanced liver fibrosis in chronic hepatitis B patients. Hong Kong Med J 2014;20(Suppl 5):31.
3. Liu SS, Chan KK, Leung RC, et al. Human papillomavirus status in southern Chinese women. Hong Kong Med J 2014;20(Suppl 5):35-8.

Use of humanised mice to study antiviral activity of human γδ-T cells against influenza A viruses

WW Tu *, YL Lau, JSM Peiris

KEY MESSAGES

1. Phosphoantigens could protect against influenza A (H1N1) virus infection in humanised mice with a human immune system.
2. This protection was strain-dependent for avian influenza A (H5N1) virus infection.
3. This suggests a novel therapeutic approach against influenza by using phosphoantigens to inhibit influenza A virus infection.
4. The humanised mouse model provides a low-cost platform for further studies of vaccines, stem cell biology, and therapeutics for human pathogens.

Hong Kong Med J 2014;20(Suppl 6):S4-6
RFCID project number: 07060482

[1] **WW Tu ***, [1] **YL Lau**, [2] **JSM Peiris**

The University of Hong Kong:
[1] *Department of Paediatrics and Adolescent Medicine*
[2] *Department of Microbiology*

* Principal applicant and corresponding author: wwtu@hku.hk

Introduction

Influenza A virus can cause substantial morbidity and mortality. Potential emergence of a new pandemic strain (eg avian influenza A virus [H5N1]) through natural reassortment is a concern. Both innate and adaptive immune systems play critical roles in protecting against influenza A viruses, and direct manipulation of the host immune system can help protect against influenza A virus infections. Vaccines targeting the adaptive immune system may be less effective against a new pandemic strain. The currently available neuraminidase inhibitors may become ineffective with the emergence of resistant virus strains. Therefore, activating early innate responses enables protection against influenza A virus infection early after virus exposure.

As the first line of the host defence, the antiviral activities of γδ–cells against other viruses have been demonstrated in different models.[1-3] Human Vδ2–T cells, representing most peripheral blood and lymphoid organ γδ–T cells, can be selectively activated and expanded by a phosphoantigen such as isopentenyl pyrophosphate, which also triggers γδ–T cells to produce interferon-γ and other cytokines and chemokines as antiviral activities.[2,3] In human in vitro systems, phosphatidic acid–activated Vδ2–T cells can inhibit virus replication and kill virus-infected cells caused by hepatitis C virus and severe acute respiratory syndrome coronavirus.[4,5] Whether phosphoantigen-activated Vδ2–T cells have antiviral activities against human and avian influenza A viruses in vivo remains unknown.

Unlike other cells in humans, Vδ2–T cells are the dominant γδ–T cells in the circulation, whereas murine γδ–T cells do not express the homologue of the Vγδ–T-cell receptor, and no functional equivalent for these cells has been identified in mice so far. Studies on non-human primates are constrained by high costs, limited availability, paucity of genetic models for human diseases, and lack of genetically inbred strains suitable for cell transplantation. Creation of humanised mice that carry partial or complete human immune systems may help to overcome these obstacles. In this study, conducted from August 2007 to July 2009, a humanised mouse model was established to investigate the antiviral activities of human T cells against human and avian influenza A viruses in vivo.

Methods

Generation of humanised mice

C57BL/10SgAiRag2$^{-/-}$γc$^{-/-}$ mice (Taconic, Hudson, NY, USA) were kept in individual ventilated cages in the Laboratory Animal Unit of the University of Hong Kong. To establish humanised mice models, human peripheral blood mononuclear cells (huPBMCs) were obtained from healthy donors after approval by the Institutional Review Board of the University of Hong Kong/Hospital Authority Hong Kong West Cluster. Humanised mice were then established as previously described with some modifications.[6] All manipulations were in compliance with the guidelines for the use of experimental animals.

Infection of humanised mice with human and avian influenza A virus

Under anaesthesia, 10-week-old humanised mice

were infected intranasally with the human influenza A virus H1N1 (A/Hong Kong/54/98) [25 μL, $10^{8.4}TCID_{50}$], mouse-adapted influenza H1N1 (A/PR/8/34) [25 μL, $1\times LD_{50}$], and avian influenza H5N1 (A/Hong Kong/483/97) or (A/Hong Kong/486/97) [25 μL, $1\times LD_{50}$]. The weight and survival of the infected mice were checked daily post-infection.

Virus titre determination and immunohistochemistry assays

The lungs of infected humanised mice were harvested at the indicated time and homogenised with phosphate buffered saline (PBS) 2 mL, and the virus titre was determined as described previously.[7] Lung immunohistochemistry staining was performed as described previously.[8]

Treatment of virus-infected humanised mice

Humanised mice were separated into mock, PBS-treated, and drug-treated groups, matched according to sex, age, and the source of huPBMCs. Four weeks after transplantation of huPBMCs, $Rag2^{-/-}\gamma c^{-/-}$ and established humanised mice were infected intranasally with human influenza H1N1 virus, PR/8 virus, or avian influenza H5N1 (25 μL, $1\times LD_{50}$) under anaesthesia. For human H1N1 and PR/8 virus infections, phosphoantigen or an equivalent volume of PBS was injected intraperitoneally on days 3, 5, 7, and 9 after virus infection, whereas for avian influenza H5N1 infection, injections were on days 1, 3, 5, 7, and 9 after virus infection. Survival was monitored and the infected mice were weighed daily; mice with >25% weight loss were sacrificed and counted as dying.

Results

Phosphoantigen-activated cells could efficiently kill human and avian influenza H1N1, H9N2, and H5N1 virus-infected cells and inhibited virus replication in vitro.[9] We tried to establish the humanised mouse model with a human immune system. Using immunodeficient C57BL/6$Rag2^{-/-}\gamma c^{-/-}$ mice that lack functional T, B, and natural killer (NK) cells, after 4 weeks of transplantation of huPBMCs, around 80% of nucleated cells in peripheral blood were human lymphoid cells expressing human CD45 and >20% expressed human CD3. Within lymphocytes, cell subsets were composed of human T cells (69.4%), B cells (5.5%), NK cells (20.0%), and T cells (2.8%). Human $CD3^+$ T cells were found in spleen, liver, and intestine, but not in lung or kidney of humanised mice at 4 weeks post-transplantation. In addition, human immunoglobulin G could be detected in the humanised mice. The humanised mice could survive for >1 year after human immune system reconstitution.

Using the humanised mouse model, the role of γδ–T cells in influenza A virus infection was determined in vivo. C57BL/10SgAi$Rag2^{-/-}\gamma c^{-/-}$ mice were transplanted with huPBMCs or γδ–T cell–depleted PBMCs. Four weeks later, humanised mice were infected intranasally with human H1N1 influenza A virus. The weight of humanised mice were monitored. Although the weight of humanised mice decreased significantly after infection, there was no significant difference in the weight of humanised mice transplanted with huPBMCs or γδ–T cell–depleted PBMCs, which indicated that unexpanded γδ–T cells had little effect on influenza A virus infection.

The number of Vδ2-T cells could be increased 8-fold after 2 days of phosphoantigen treatment. This suggested that phosphoantigen could expand human Vδ2-T cells in vivo.

To determine whether phosphoantigen could be used for treatment of human influenza A virus infection in a humanised mouse model, the effect of phosphoantigen treatment on human influenza H1N1 virus infection in vivo was examined. During 20 days of observation, humanised mice could be effectively infected by human influenza H1N1 virus as indicated by the significant weight loss. However, for humanised mice treated with phosphoantigen, the weight did not decrease at all during this period. The phosphoantigen treatment significantly inhibited virus replication in the lung compared with the control group. Similarly, phosphoantigen treatment significantly decreased weight loss and mortality, and reduced virus titres in the lung infected with mouse-adapted influenza H1N1 PR/8 virus.

Similar to observations in humanised mice infected with influenza H1N1 virus, treatment with phosphoantigen significantly decreased weight loss and mortality, and reduced virus titres in the lung infected with highly pathogenic avian influenza H5N1 virus (A/Hong Kong/486/97). However, phosphoantigen had no protective role against another highly pathogenic avian influenza H5N1 virus infection (A/Hong Kong/483/97); all the humanised mice died 9 days after avian influenza H5N1 virus infection.

Discussion

Using a humanised mouse model, phosphoantigen was demonstrated to control human influenza A virus infection in vivo. For avian influenza A virus infection, this protection was strain-dependent. Phosphoantigen could control avian influenza A H5N1/486 but not H5N1/483 virus infection in vivo. The control of influenza A virus infection may be mediated by the selective activation and expansion of human Vδ2-T cells in the humanised mouse model. This variance between the different strains of H5N1 virus may be explained by the fact that H5N1/483 virus can invade mouse brain and

cause death, but the human Vδ2-T cells cannot cross the brain-blood barrier. Our study suggests a novel therapeutic approach against influenza by using phosphoantigens to activate and expand γδ–T cells against influenza infection.

Acknowledgements

This study was supported in part by the Research Fund for the Control of Infectious Diseases, Food and Health Bureau, Hong Kong SAR Government (#07060482); University Grants Committee, (AoE/M-12/06); and Research Grants Council (General Research Fund, HKU 777108M).

References

1. Born WK, Reardon CL, O'Brien RL. The function of gammadelta T cells in innate immunity. Curr Opin Immunol 2006;18:31-8.
2. Poccia F, Agrati C, Martini F, Capobianchi MR, Wallace M, Malkovsky M. Antiviral reactivities of gammadelta T cells. Microbes Infect 2005;7:518-28.
3. Poccia F, Agrati C, Martini F, Mejia G, Wallace M, Malkovsky M. Vgamma9Vdelta2 T cell-mediated non-cytolytic antiviral mechanisms and their potential for cell-based therapy. Immunol Lett 2005;100:14-20.
4. Agrati C, Alonzi T, De Santis R, et al. Activation of Vgamma9Vdelta2 T cells by non-peptidic antigens induces the inhibition of subgenomic HCV replication. Int Immunol 2006;18:11-8.
5. Poccia F, Agrati C, Castilletti C, et al. Anti-severe acute respiratory syndrome coronavirus immune responses: the role played by V gamma 9V delta 2 T cells. J Infect Dis 2006;193:1244-9.
6. Berney T, Molano RD, Pileggi A, et al. Patterns of engraftment in different strains of immunodeficient mice reconstituted with human peripheral blood lymphocytes. Transplantation 2001;72:133-40.
7. Meguro H, Bryant JD, Torrence AE, Wright PF. Canine kidney cell line for isolation of respiratory viruses. J Clin Microbiol 1979;9:175-9.
8. Dahl ME, Dabbagh K, Liggitt D, Kim S, Lewis DB. Viral-induced T helper type 1 responses enhance allergic disease by effects on lung dendritic cells. Nat Immunol 2004;5:337-43.
9. Qin G, Mao H, Zheng J, et al. Phosphoantigen-expanded human gammadelta T cells display potent cytotoxicity against monocyte-derived macrophages infected with human and avian influenza viruses. J Infect Dis 2009;200:858-65.

Avian influenza A H5N1 infection on human cellular microRNA profile: identification of gene regulatory pathway

PKS Chan *, KF To, WY Lam

KEY MESSAGES

1. Based on the broad-catching microRNA (miRNA) microarray approach, dysregulation of miRNA expression is mainly observed in highly pathogenic avian influenza A (H5N1) virus infection.
2. miRNA 141 (miR-141) was induced shortly after influenza A (H1N1) virus infection. Induction was greater in H5N1 infection than in seasonal H1N1 infection.
3. A cytokine, transforming growth factor-β2, which plays an important role in regulating inflammatory processes, was identified as a target of miR-141 binding. This suggests that influenza A virus infection, in particular highly pathogenic H5N1, can affect the inflammatory processes via miR-141 induction.

Hong Kong Med J 2014;20(Suppl 6):S7-10
RFCID project number: 08070022

[1,2] **PKS Chan *, [3] KF To, [1] WY Lam**

The Chinese University of Hong Kong:
[1] *Department of Microbiology*
[2] *Stanley Ho Centre for Emerging Infectious Diseases*
[3] *Department of Anatomical and Cellular Pathology, Faculty of Medicine*

* Principal applicant and corresponding author: paulkschan@cuhk.edu.hk

Introduction

Avian influenza remains a threat to poultry and human health. From December 2003 to March 2011, more than 534 human infections and 316 deaths were reported to the World Health Organization. Outbreaks of avian influenza A (H5N1) virus infection in poultry have swept Southeast Asia and many other parts of the world. Cytokine storm and reactive haemophagocytic syndrome are the key features to distinguish H5N1 infection from seasonal influenza A (H1N1) virus infection.[1-3]

MicroRNAs (miRNAs) are a new class of 18-23 nucleotide non-coding RNAs that play critical roles in a wide spectrum of biological processes. MiRNA is one of the major gene regulatory families in eukaryotic cells.[4,5] However, the functions of most of the identified miRNAs remains unknown. The miRNA pathway exists in viral species, indicating that the host miRNAs may also have a direct or indirect regulatory role on viral replication.

This study was conducted from December 2008 to November 2010 and aimed to elucidate how H5N1 infection disturbs the human gene regulatory pathways leading to adverse pathological events. We hypothesised that miRNAs could be involved in the influenza virus infection response.

Materials and methods

Infection of cell culture with influenza A viruses

The H5N1 virus (A/Hong Kong/483/1997) was isolated from a patient with fatal infection in Hong Kong in 1997, and the H5N1 virus (A/Thai/KAN1/2004) was isolated from a patient with fatal infection in Thailand in 2004. For comparison, a human H1N1 strain isolated in 2002 (A/HongKong/CUHK-13003/2002) was included. NCI-H292 cells were grown to confluence in sterile T75 tissue culture flasks for the inoculation of virus isolate at a multiplicity of infection of one.

RNA extraction and miRNA expression profiling

Total RNA was extracted from normal and infected NCI-H292 cells using Trizol reagent (Invitrogen; Life Technologies, Carlsbad, CA, USA) following the manufacturer's protocol. MiRNAs were labelled using miRNA labelling reagent (Agilent Technologies, Santa Clara, CA, USA) and hybridised to human miRNA arrays (Agilent Technologies) according to the manufacturer's protocol. Each miRNA array facilitated us to interrogate 866 human miRNAs. The results were analysed using Genespring GX 10.0.2 software (Agilent Technologies).

TaqMan real-time RT-PCR for quantification of miRNAs

Total RNA was reversely transcribed with looped miRNA-specific real-time primers provided in the TaqMan MicroRNA Assays (Applied Biosystems, Foster City, CA, USA). Each cDNA was amplified with sequence-specific TaqMan MiRNA Assays. All

samples were tested in triplicate and were compared with the threshold cycle obtained from 18S rRNA assay (Applied Biosystems) for the normalisation of total RNA input.

qRT-PCR for quantification of TGF-β2 miRNA level and enzyme-linked immunosorbent assay measurement of TGF-β2 protein level

Total RNA extracted from cell cultures was reversely transcribed to cDNA using the poly(dT) primers and SuperScript III Reverse Transcriptase (Invitrogen), and quantified by real-time PCR. Expression of the β-actin gene was also quantified in a similar way for normalisation. The comparative delta-delta C_T method was used to analyse the results. Cell culture supernatant was collected at 24 hours post-infection for the analysis of TGF-β2 expression using enzyme-linked immunosorbent assay (Emax ImmunoAssay Systems, Promega, Madison, WI, USA).

Reverse transfection of a mimic and an inhibitor of miRNA-141

The cells were transfected in suspension after trypsinisation with 60 nM anti-miR, pre-miR, or a negative control (Applied Biosystems). At 24 hours post-transfection, the cells were lysed for qRT-PCR analysis or subjected to either H1N1 or H5N1 virus infection.

Results

A list of differentially expressed miRNA was identified for H1N1 and H5N1 subtypes, and the temporal pattern of expression was delineated. Among the listed profiles of differentially regulated miRNA, miR-1246, miR-663, and miR-574-3p were up-regulated (>3-fold) at some time points during the course of infection with H5N1, compared with the non-infected control cells. Moreover, miR-100*, miR-21*, miR-141, miR-1274a, and miR1274b were highly down-regulated (>3-fold) in infection with H5N1, particularly at 18 or 24 hours post-infection, compared with the non-infected control cells. Similar miRNA profiles were also observed in H1N1 infection, but the magnitude of changes (<2-fold) was much lower than that in H5N1 infection.

The targets were predicted using the TargetScan computer software (http://www.targetscan.org/). There was a 3'UTR binding site on TGF-β2 for miR-141. miR-141 was initially up-regulated at 3 hours post-infection, which was higher in H5N1 infection (5- to 14-fold) than in H1N1 infection (2- to 3-fold) [Fig 1].

Using ectopic expression of miR-141, the level of TGF-β2 mRNA was significantly decreased in miR-141 transfected cells but not in negative-control miRNA-mimicking transfected cells (Fig 2).

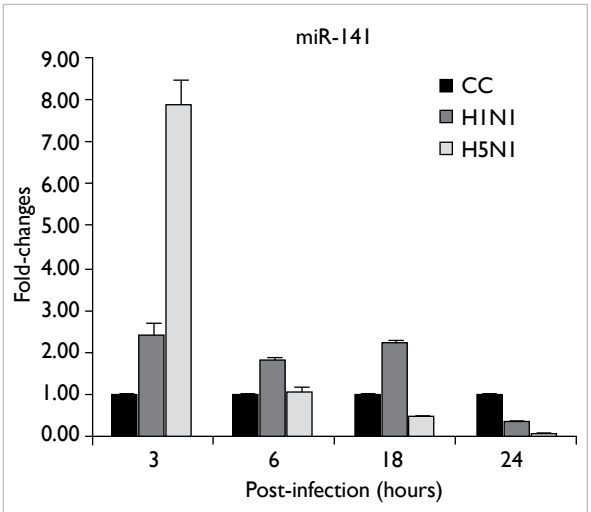

FIG 1. Patterns of changes in cellular microRNA (miR)-141 expression after influenza A virus infection. NCI-H292 cells are infected with influenza A virus subtypes (H1N1/2002, H5N1/2004 viruses) at a multiplicity of infection of one. qRT-PCR is used to quantify the miR-141 levels, and fold-changes are calculated by the ΔΔCT method compared with non-infection control cells using 18S rRNA level for normalisation.

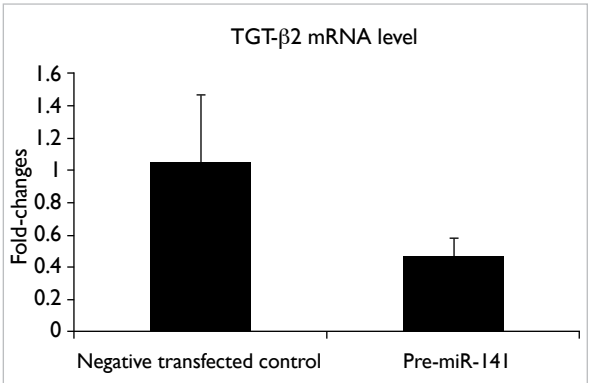

FIG 2. The TGF-β2 3'UTR is regulated by microRNA (miR)-141. NCI-H292 cells are transfected with pre-miR-141 and negative control. The fold-changes of mRNA level of TGF-β2 are measured by qRT-PCR at 24 hours after transfection. Fold-changes are calculated by the ΔΔCT method compared with negatively transfected control cells using β-actin level for normalisation.

The functional relevance of changes in miRNA-141 expression during influenza A virus infection was then assessed using anti-miR miRNA inhibitors. The anti-miR miR-141 inhibitor could cause an increase in TGF-β2 protein expression in H1N1 or H5N1 infected cells (Fig 3), compared with cells only infected with H1N1 or H5N1 without anti-miR miR-141 inhibitor treatment.

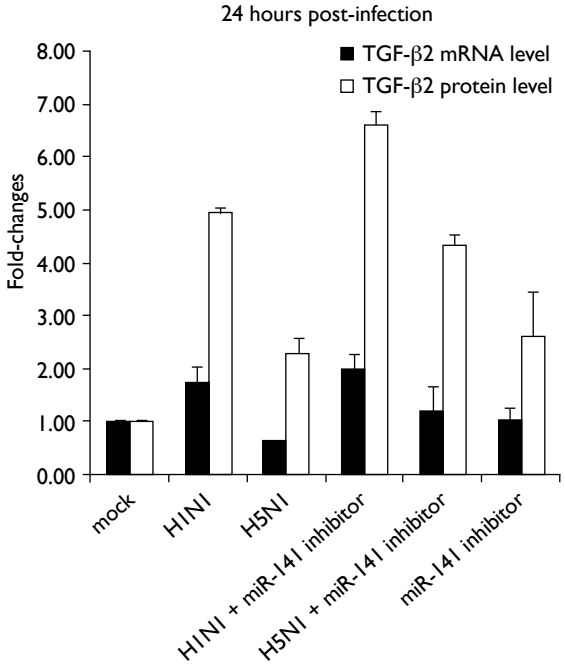

FIG 3. Measurement of TGF-β2 mRNA and protein level.
NCI-H292 cells, with or without treatment with microRNA (miR)-141 inhibitor, are infected with influenza A virus subtypes (H1N1/2002, H5N1/2004 viruses) at a multiplicity of infection of one for 24 hours. qRT-PCR is used to quantify the TGF-β2 mRNA levels, and fold-changes are calculated by the ΔΔCT method compared with non-infection control cells (mock) using endogeneous actin mRNA level for normalisation. The TGF-β2 protein level is measured by enzyme-linked immunosorbent assay compared with mock.

Discussion

In this study, influenza A virus infection altered the regulation of cellular miRNAs; the extent was greater in H5N1 infection than in H1N1 infection. The expression of miR-141 was affected by influenza A virus infection. The altered miR-141 expression then affected the expression of the cytokine TGF-β2. In fact, the miR-141 is a member of the miR-200 family (miR-200a, miR-200b, miR-200c, miR-141, and miR-429). Previous studies of miR-141 mainly involved its role in cancer; miR-141 was markedly down-regulated in cells that had undergone epithelial to mesenchymal transition in response to TGF-β, and was overexpressed in ovarian and colorectal cancers and down-regulated in prostate, hepatocellular, renal cell, and gastric cancer tissues. This raises a controversy about the role of miR-141 in cancer progression. Furthermore, the miR-200 family members have roles in maintaining the epithelial phenotype of cancer cells. A member of this family—miR-200a—was differentially expressed in response to influenza virus infection in another study. The targets of miR-200a are associated with viral gene replication and the JAK-STAT signalling pathway, which is closely related to the type 1 interferon-mediated innate immune response. However, the effect of miR-141 on virus infection is not known, except that enterovirus can induce miR-141 and contribute to the shut-off of host protein translation by targeting the translation initiation factor eIF4E.

In addition, influenza A virus infection reduces or promotes the expression of the host miR-141 in a time-dependent manner. In this study, TGF-β2 mRNA was suppressed in miR-141 overexpressed cells. This is in line with another study showing that the 3'UTR of TGF-β2 mRNA contains a target site for miR-141/200a, and the expression of TGF-β2 was significantly decreased in miR-141/200a transfected cells. Furthermore, miR-141 may not only work as translational repressors of target mRNAs, but also cause a decrease in TGF-β2 mRNA levels. These findings are similar to recent data demonstrating that some miRNAs can alter the mRNA levels of target genes. This ability is probably independent of the ability of these miRNAs to regulate the translation of target mRNAs.

In this study, antagomiR-141 moderately increased the accumulation of TGF-β2 protein during influenza A virus infection. This might be because, by the use of anti-miR miR-141 inhibitor that decreases the cellular pool of miR-141, the translation control of the TGF-β2 mRNA was subsequently released and caused the TGF-β2 protein to express and accumulate during influenza A virus infection. H1N1 was the only subtype that could induce a sustained increase in TGF-β2 at the protein level. H1N1 infection induced a small amount of miR-141 expression, whereas H5N1 infection induced a higher amount of miR-141 expression in the early phase of infection. As a consequence of the higher amount of miR-141 in H5N1 infection, TGF-β2 expression might be more greatly reduced than in H1N1 infection. TGF-β2 plays a vital role in T-cell inhibition, as it can act as both an immunosuppressive agent and a potent proinflammatory molecule through its ability to attract and regulate inflammatory molecules. Furthermore, TGF-β2 inhibits T helper 1 cytokine-mediated induction of CCL-2/MCP-1, CCL-3/MIP-1α, CCL-4/MIP-1β, CCL-5/RANTES, CCL-9/MIP-1γ, CXCL-2/MIP-2, and CXCL-10/IP-10. Moreover, the pro-inflammatory responses during influenza A virus infection are tightly controlled by anti-inflammatory mediators such as TGF-β2 to protect the easily damaged lung tissue from destructive side effects of virus-induced inflammation. Therefore, the down-regulation of TGF-β2 protein by miR-141 may be an important step in the excessive inflammation progression during influenza A virus infection, particularly in H5N1 infection. However, whether the recovery of TGF-β2 expression by anti-miR miR-141

inhibitor could resolve the hypercytokinaemic stage of H5N1 infection needs to be further studied.

One limitation of this study was that the roles of other miRNAs whose expression was also altered after infection by influenza A virus were not assessed. The miRNA microarrays used did not contain probes for every known miRNA; thus it is possible that influenza A virus infection affects the expression of some other miRNAs not yet studied. The virus may interact with miRNA regulatory pathways differently in other cell or tissue types, or in other physiological states.

Conclusion

Based on the broad-catching miRNA microarray results, dysregulation of miRNA expression was mainly observed in highly pathogenic H5N1 infection. miR-141 was induced at an early phase of influenza A virus infection; the induction was higher in H5N1 infection than in H1N1 infection. Moreover, TGF-β2, which plays an important role in regulating inflammatory processes, was identified as a target of miR-141 binding. As a result, influenza A virus infection could affect the inflammatory processes via miR-141 induction.

Acknowledgement

The study was supported by the Research Fund for the Control of Infectious Diseases, Food and Health Bureau, Hong Kong SAR Government (#08070022).

References

1. Chan PK. Outbreak of avian influenza A(H5N1) virus infection in Hong Kong in 1997. Clin Infect Dis 2002;34(Suppl 2):S58-64.
2. Peiris JS, Yu WC, Leung CW, et al. Re-emergence of fatal human influenza A subtype H5N1 disease. Lancet 2004;363:617-9.
3. Yuen KY, Chan PK, Peiris M, et al. Clinical features and rapid viral diagnosis of human disease associated with avian influenza A H5N1 virus. Lancet 1998;351:467-71.
4. Muller S, Imler JL. Dicing with viruses: microRNAs as antiviral factors. Immunity 2007;27:1-3.
5. Rane S, Sayed D, Abdellatif M. MicroRNA with a MacroFunction. Cell Cycle 2007;15:1850-5.

Role of toll-like receptors in naturally occurring influenza virus infection

NLS Lee *, CK Wong, DSC Hui, PKS Chan

KEY MESSAGES

1. In naturally occurring influenza virus infection, there is differential increase in toll-like receptor (TLR) expression in antigen-presenting cells.
2. Increased TLR expression is associated with early innate suppression of virus, reducing influenza viral loads.
3. Concomitantly, TLR signalling induces pro-inflammatory and adaptive cytokine responses.
4. Targeting of TLRs may be a novel strategy to improve influenza control.

Hong Kong Med J 2014;20(Suppl 6):S11-5
RFCID project number: 09080102

[1,2] **NLS Lee *, [3] CK Wong, [1,2] DSC Hui, [2,4] PKS Chan**

The Chinese University of Hong Kong:
[1] *Department of Medicine and Therapeutics*
[2] *Stanley Ho Centre for Emerging Infectious Diseases*
[3] *Department of Chemical Pathology*
[4] *Department of Microbiology, Faculty of Medicine*

* Principal applicant and corresponding author: leelsn@cuhk.edu.hk

Introduction

Toll-like receptors (TLRs) are pattern recognition receptors expressed by antigen-presenting dendritic cells, monocytes/macrophages, and epithelial cells; when activated, they trigger the innate immune responses. Viral nucleic acids (dsRNA, ssRNA, CpG oligodeoxynucleotides) are detected by the endosomal TLRs 3,7,8, and 9, whereas bacterial components (peptidoglycans/lipoproteins, lipopolysaccharides) are detected by cell-surface TLRs 2 and 4. In influenza pathogenesis, TLRs induce expressions of type-I interferons and pro-inflammatory cytokines (eg IL-6, TNF-α), limiting viral replication/dissemination, mediating tissue inflammation, and linking to adaptive immunity development. Animal models suggested that TLR targeting may be clinically useful, as it can rapidly up-regulate innate immunity and provide broad-range virus strain non-specific protection against lethal influenza virus challenge. This study hypothesised that the 'virus-sensing' TLRs are up-regulated in patients with influenza virus infections, and TLR signalling pathway activation is associated with virus inhibition and pro-inflammatory cytokine expression. Adults hospitalised with influenza virus A infection were compared with healthy controls, and TLR expression in antigen-presenting cells, respiratory tract viral loads, plasma cytokines/chemokines, and signalling molecules were studied simultaneously. Patients' immune effector cells were stimulated ex vivo with TLR-specific ligands for response.

Methods

This prospective, case-control study was conducted from January 2010 to December 2011 during the influenza seasonal peaks in Hong Kong. Informed consent was obtained from each subject. Ethical approval was obtained from the Institutional Review Boards of the Chinese University of Hong Kong and the Hospital Authority of Hong Kong. Adults aged 18 years or older who were hospitalised for influenza A virus infection and presented within 48 hours of illness onset were recruited. Patients with antiviral treatment before enrolment, underlying immunocompromised conditions (eg autoimmune diseases, HIV/AIDS) or receiving immunosuppressant (including corticosteroids) were excluded. Age- and sex-matched controls were recruited outside the seasonal peak periods from the general outpatient clinics and the community for comparison. Those with any immunocompromised condition or a history of any febrile illness in the past 4 weeks were excluded.

Peripheral blood samples were taken. Expression profiles of TLRs 2, 3, 4, 7, 8, and 9 on blood monocytes (CD14+), 'total' dendritic cells (CD14-, CD16-, CD85k+), myeloid dendritic cells (CD16-, CD14-, CD85k+, CD123-) and plasmacytoid dendritic cells (CD16-, CD14-, CD85k+, CD123+) were analysed by flow cytometry using established methods. Intracellular signalling molecule expression on peripheral blood mononucleated cells (PBMCs), including activated MAPKs (phospho-p38 and phospho-ERK) and NF-κB (phospho-IκB) were similarly analysed by flow cytometry. Plasma concentrations of 14 'pro-inflammatory' or 'adaptive' immunity-related cytokines/chemokines, including IL-6, TNF-α, CXCL8/IL-8, CCL2/MCP-1, and IL-1β; and IFN-γ, CXCL10/IP-10, CXCL9/MIG,

CCL5/RANTES, and IL-12p70; and IFN-α2, CCL3/MIP-1α, IL-10, and sTNFR-1 (indicating TNF-α release) were measured using cytometric bead array with flow cytometry analysis or using enzyme-linked immunosorbent assay as previously described. PBMCs obtained from recruited participants were cultured and stimulated with TLR-specific ligands to assess their response for cytokine/chemokine production (compared with 'control medium'). These included peptidoglycan (TLR2-ligand), polyinosinic-polycytidylic acid (TLR3-ligand), ultra-purified lipopolysaccharide (TLR4-ligand), R837/Imiquimod (TLR7-ligand), ssRNA (TLR8-ligand), and CpG DNA (TLR9-ligand).

All nasopharyngeal samples collected at presentation were subjected to influenza virus detection using immunofluorescence or PCR assays for diagnosis; virus isolation was performed in parallel. Real-time reverse-transcriptase PCR assay (targeting M-gene) was performed on the original specimens to determine viral RNA concentration (copies/μL RNA) using established methods.

Results

A total of 42 patients hospitalised with influenza virus (A/H3N2, n=24; A/H1N1pdm09, n=18) and 20 controls were enrolled. Patients and controls were similar in terms of age (67.7±15.9 years vs 62.0±13.5 years, P>0.05) and sex distribution (male: 57% vs 55%, P>0.05). Among patients, 81% developed acute respiratory and/or cardiovascular complications, and 50% required supplemental oxygen therapy because of hypoxaemia. Four (9.5%) patients developed critical illness requiring ventilatory support, and one died.

Levels of expression of 'virus sensing' TLRs 3, 7, 8, and 9 and 'bacterial sensing' TLRs 2 and 4 in monocytes and dendritic cells were compared between patients and controls. Patients' blood samples were collected at a median of 2 (interquartile range, 1-2) days from symptom onset, prior to antiviral treatment. Expression of TLRs 8 and 9 increased significantly, but that of TLRs 2 and 4 was suppressed (Fig 1). There were trends for increased expression of TLRs 3 and 7 in the dendritic cells. Subgroup analyses of plasmacytoid and myeloid dendritic cells showed similar results. A/H3N2 and A/H1N1pdm09 virus infections did not differ significantly in terms of TLR expression profile and magnitude (monocytes and dendritic cells, all P≥0.1).

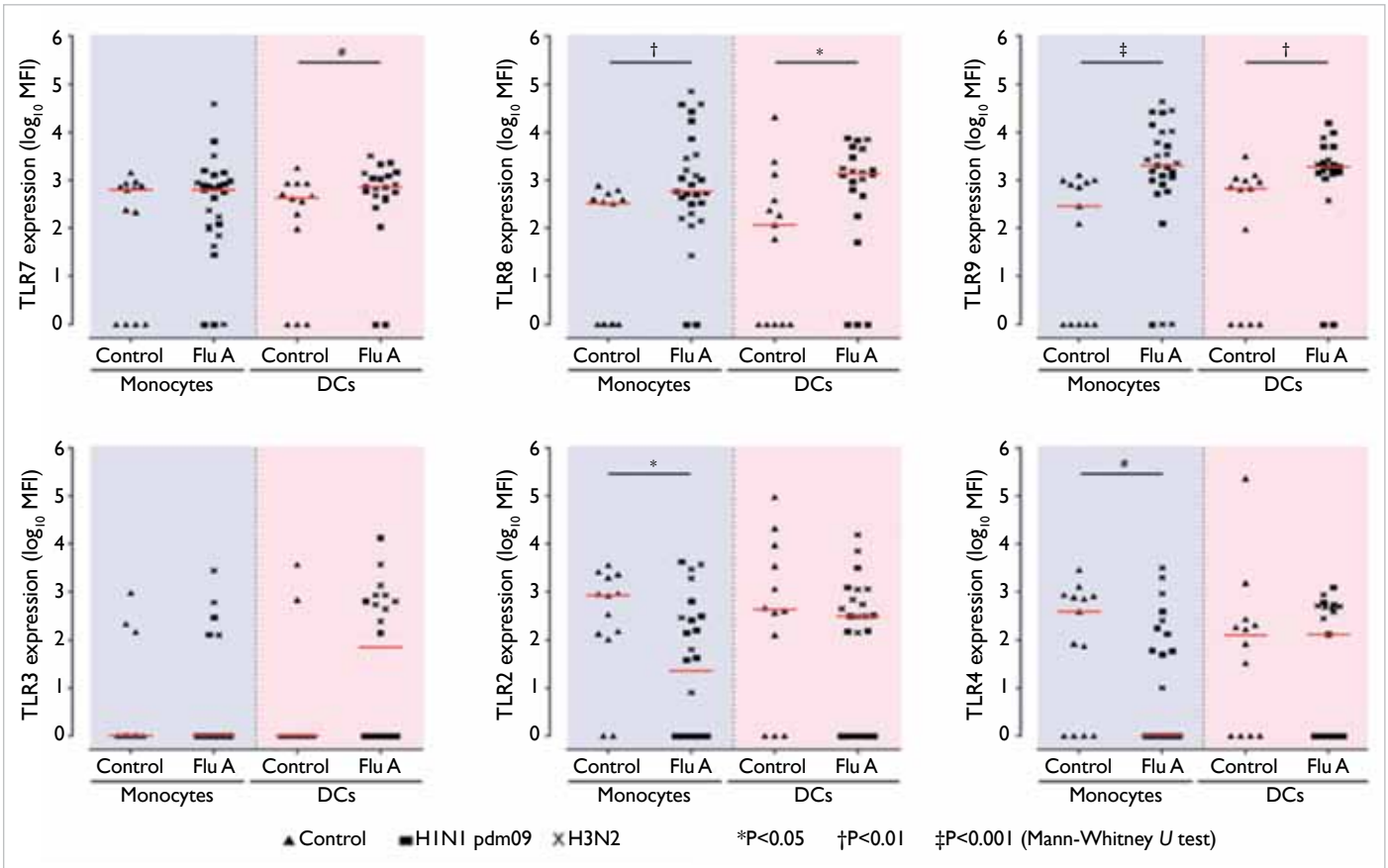

FIG 1. Expressions of toll-like receptors (TLRs) in terms of mean fluorescence intensity (MFI) in monocytes and dendritic cells (DCs) in influenza patients and controls: values are represented in logarithmic scale; horizontal bars represent median values

The relationship between nasopharyngeal viral RNA concentration ('viral load') at time of presentation and TLR expression level in influenza patients was examined (Fig 2). There were significant negative correlations between TLR 3, 8, and 9 expression levels and viral load (ie a lower level of TLR expression was associated with a higher viral load), particularly for the dendritic cells. Similar trends were shown for TLR7. Multivariate linear regression analysis showed that a higher viral load was independently associated with a more severe illness as indicated by pneumonia and hypoxaemia (β=+0.80; standard error [SE], 0.37; 95% confidence interval [CI], 0.05 to 1.55; P=0.037), adjusted for time elapsed from onset (β=-0.37; SE, 0.16; 95% CI, -0.70 to -0.04; P=0.029) and virus strain (β=+0.60; SE, 0.33; 95% CI, -0.07 to +1.26; P=0.076). Although TLRs 2 and 4 were generally suppressed, in several patients with culture-confirmed bacterial superinfection, these were up-regulated; TLRs 3, 7, 8, and 9 were unaffected.

Relationships between levels of expressions of TLR, signalling molecules, and plasma cytokines were examined. Increased cellular expression of TLRs 7, 8, and 9 correlated with increased plasma levels of proinflammatory cytokines, including IL-6, soluble TNF receptor-1 (indicating TNF-α release), CXCL8/IL-8, CCL2/MCP-1, and the adaptive cytokines IFN-γ, CXCL10/IP-10, and CXCL9/MIG (Spearman's *rho*, +0.30 to +0.49; all P<0.05). Increased TLR expression was also shown to correlate with increased intracellular signalling molecules phospho(p)-IκB, pp38-MAPK, and pERK (Spearman's *rho*; +0.49 to +0.63; all P<0.05).

These in vivo findings were supported by the ex vivo experiment results that showed a significant difference between patients and controls in their PBMCs' cytokine responses towards TLR-specific ligand activation (Table 1). For instance, stimulation of the TLR9 signalling pathway resulted in smaller increases in IL-6, TNF-α, CXCL10/IP-10, and IFN-α from baseline in patients than in controls, but

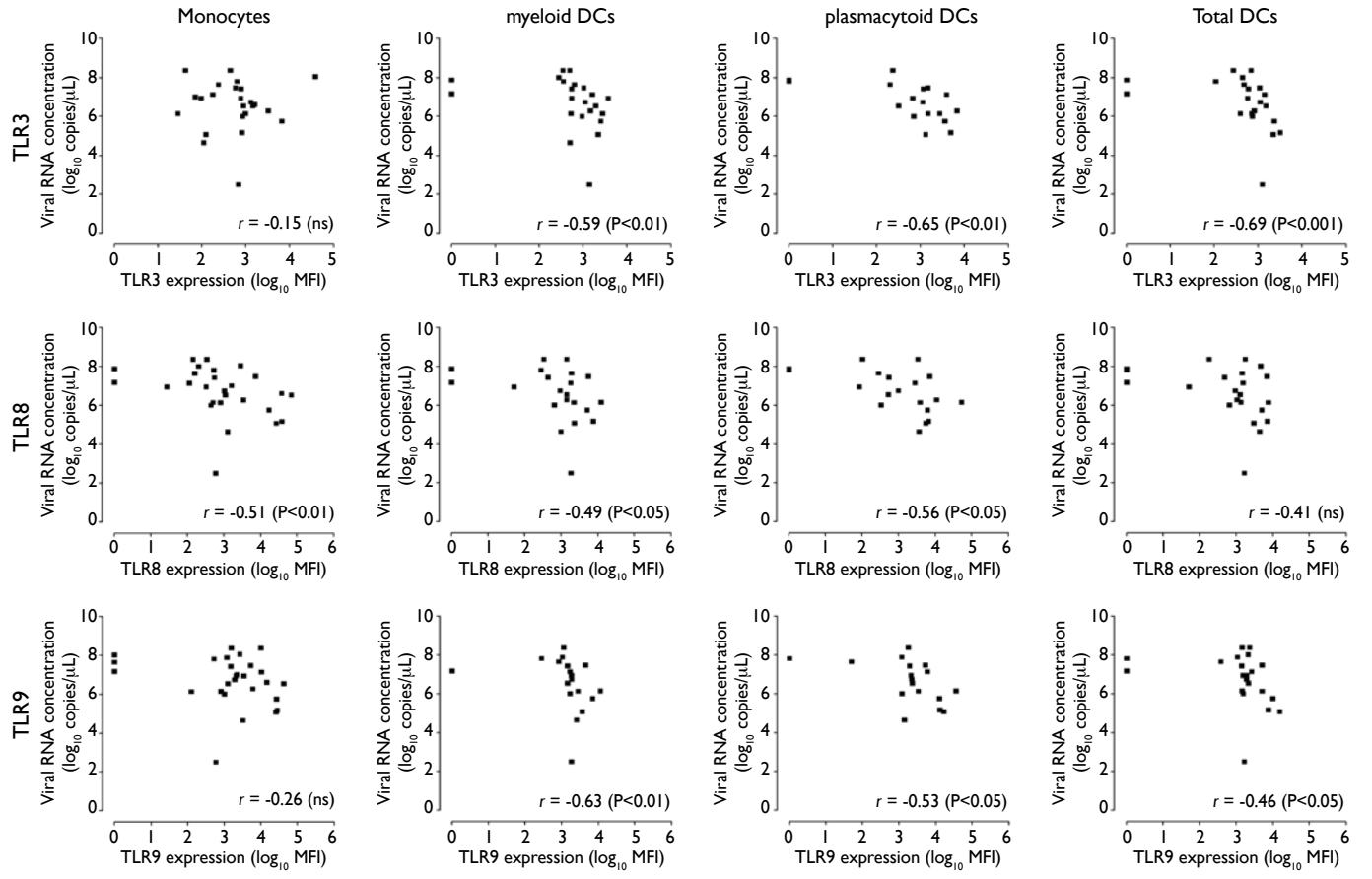

FIG 2. Negative correlations between expressions of toll-like receptors (TLRs) and influenza viral load in the respiratory tract: values are represented in logarithmic scale; trends of negative correlation between viral RNA concentration and TLR7 expression are also observed: 'total' dendritic cells [DC] (*r*= -0.34, P=0.12), plasmacytoid DCs (*r*= -0.31, P=0.21), and myeloid DCs (*r*= -0.34, P=0.18)

TABLE. Ex vivo cytokine/chemokine response of peripheral blood mononucleated cells (PBMCs) to toll-like receptor (TLR)-specific ligands in influenza patients and controls: in convalescent-phase samples from six influenza patients, median (interquartile range) fold-change for TLR9 ligand: IL-6 (4.8 [1.2-7.1]), TNF-α (2.4 [1.0-4.2]), CXCL10/IP10 (18.6 [0.8-34.5]), IL-10 (1.8[1.1-2.7]), IFN-α (2.1[1.2-39.4]), for TLR7 ligand: IL-6 (2.1 [0.7-42.7]), TNF-α (1.4 [1.0-3.9]), CXCL10/IP-10 (1.0 [1.0-5.3]), IL-10 (1.0 [0.9-1.7]), time interval from acute-phase samples (9 [7-14] days)

TLR-specific ligand activation	IL-6	TNF-α	CCL2 (MCP-1)	CXCL10 (IP-10)	IFN-γ	IL-10	IFN-α
TLR3 (PolyIC)							
Patients	99.5 (26.4-390.6)	101.0 (24.3-374.0)	4.0 (1.0-17.6)	1.0 (1.0-1.0)	1.5 (1.0-2.1)	39.5 (8.4-61.1)	1.0 (0.9-1.5)
Controls	84.5 (41.7-243.3)	84.6 (29.2-241.3)	1.2 (1.0-16.9)	1.0 (1.0-1.0)	1.8 (1.2-3.6)	53.2 (21.7-85.5)	1.3 (1.0-1.7)
TLR7 (Imiquimod)							
Patients	7.1 (2.6-41.6)†	1.3 (1.0-3.8)†	3.7 (1.0-16.9)	2.6 (1.0-12.4)‡	1.0 (0.8-1.5)	1.3 (1.0-2.1)*	1.2 (0.9-2.3)
Controls	4.2 (0.7-9.6)	1.0 (0.8-1.9)	1.5 (1.0-20.9)	1.0 (1.0-1.2)	1.4 (1.0-2.0)	1.0 (1.0-1.2)	1.2 (0.9-4.1)
TLR8 (ssRNA)							
Patients	2.8 (1.1-15.3)	1.5 (1.0-6.7)	1.5 (1.0-5.6)	1.0 (1.0-1.0)	1.1 (0.9-1.8)	1.0 (1.0-1.7)	1.0 (0.9-1.1)
Controls	2.9 (1.5-5.8)	2.2 (1.0-6.9)	1.0 (1.0-2.3)	1.0 (1.0-1.0)	1.0 (0.8-1.5)	1.0 (1.0-1.1)	1.0 (0.8-1.3)
TLR9 (CpG DNA)							
Patients	1.5 (0.9-3.3)*	1.0 (1.0-1.0)†	2.2 (1.0-8.2)	1.0 (1.0-3.9)‡	1.2 (1.0-1.6)	1.0 (1.0-1.0)‡	1.2 (1.0-1.3)‡
Controls	2.6 (1.6-7.0)	1.6 (1.0-2.9)	1.0 (1.0-16.9)	9.2 (1.0-27.8)	1.2 (1.0-2.2)	1.5 (1.3-2.0)	2.1 (1.3-10.5)
TLR2 (PGN)							
Patients	122.8 (25.9-390.6)	314.6 (84.5-1129.5)	3.8 (1.0-16.9)	1.0 (1.0-1.7)	1.3 (1.0-2.0)	47.7 (12.4-84.0)	1.1 (0.9-1.4)
Controls	89.8 (62.7-310.2)	278.3 (65.4-434.7)	1.3 (1.0-9.6)	1.0 (1.0-1.0)	1.4 (1.0-2.2)	32.5 (15.1-89.1)	1.5 (0.9-2.6)
TLR4 (LPS)							
Patients	118.7 (26.3-394.0)	125.4 (29.3-719.4)	3.7 (1.0-14.8)	1.0 (1.0-1.0)	1.3 (1.0-2.5)	37.3 (8.6-65.8)	1.3 (1.0-1.5)
Controls	84.5 (41.7-243.3)	96.3 (21.6-453.7)	1.2 (1.0-16.9)	1.0 (1.0-1.8)	1.5 (1.1-2.9)	49.4 (31.7-97.9)	1.1 (0.9-2.2)

* P≤0.1 using Mann-Whitney *U* test
† P≤0.05 using Mann-Whitney *U* test
‡ P≤0.01 using Mann-Whitney *U* test

such responsiveness for cytokine production was higher with TLR7 ligand binding in patients than in controls. In both cases, the responses normalised when patients' illness subsided, indicating that the TLR-signalling pathways were active during influenza virus infection. No difference was found between patients and controls for TLRs 2 or 4 ligand activation. Results were similar between influenza A/H3N2 and A/H1N1pdm09 virus infections.

Discussion

Our results on natural infections are consistent with earlier in vitro and animal studies, which showed that the 'viral sensing' TLRs 3, 7, 8, and 9 are up-regulated in antigen-presenting cells, and signal the innate virus inhibitory and inflammatory responses in influenza. TLR9 activation in dendritic cells strongly induces the release of type-1 IFNs and pro-inflammatory cytokines, and up-regulates co-stimulatory molecules (eg CD80/86); TLR7/8 activation induces IFNs, pro-inflammatory IL-6, TNF-α, CCL2/MCP-1, and CXCL8/IL-8, and promotes dendritic cell maturation; TLR3 in epithelial cells causes tissue inflammation through IL-6, TNF-α, and CXCL8/IL-8 induction and effector cell recruitment. Data in humans also showed significant increase in TLRs 8 and 9 expression, and increasing trends in TLRs 3 and 7 expression, together with highly increased inflammatory cytokines in severe influenza virus A/H1N1pdm09 infections.[1] Notably, the 'bacterial sensing' of TLRs 2 and 4 were suppressed. Their down-regulation may impair phagocyte recruitment and bacterial elimination, thus explaining the increased risk of secondary infections post-influenza. There was no significant difference in TLR expression (pattern/magnitude) between influenza virus A/H3N2 and A/H1N1pdm09 infections, unlike their adaptive immune responses. This may reflect the 'less specific' nature of innate immunity, which can be advantageous when considering TLR targeting for prophylaxis.

This study suggested that TLRs play an important role in virus control in the early phase of naturally occurring influenza. Higher expression levels of TLRs 3, 8, and 9 (and trends for TLR7) in the innate immune cells, particularly the dendritic cells, were associated with lower level of virus

replication ('viral load') in the respiratory tract for both virus strains. Reduced viral load was associated with milder illness. As all patients were studied within the first 48 hours of illness onset, these observations were unlikely to be the sole result of adaptive immunity. These results are in line with recent mice experiments in which TLR activation rapidly produced virus inhibitory responses (predominantly through type-I IFNs and IFN-stimulated mechanisms), conferring protection against influenza challenge. Aerosolised TLR9 and TLR2/6 agonists given 3 days before or shortly after lethal challenge with influenza virus A/H3N2 or A/H1N1pdm09 reduced mice lung viral titres and enhanced survival.[2] Starting intranasal TLR3 agonist pretreatment 6 hours before lethal influenza challenges reduced lung viral titres and mortality; the protection was 'broad-range' (A/H1N1, A/H3N2, A/H1N1pdm09, A/H5N1, A/H9N2).[3] Pretreatment with TLR9 and TLR3 agonists up-regulated the TLRs within hours, and protected mice against lethal influenza virus (A/H1N1, A/H3N2, A/H5N1) infections for 7 to 14 days.[4] Prophylactic TLR7/8 or TLR7 agonist administration also resulted in virus inhibition and improved mice survival. Thus, potentiating the innate antiviral responses through TLR targeting/activation may be useful in enhancing initial influenza virus control in humans.

In patients with influenza virus infection, TLR-signalling led to the inflammatory response, and linked to the adaptive response. Increased TLRs 7, 8, and 9 expression correlated with the key intracellular signalling molecules (MAPKs, NF-κB/IκB), and higher levels of pro-inflammatory cytokines (IL-6, TNF-α). TLR9 and TLR7/8 (which signal through the MyD88 pathway) were associated with the 'adaptive' cytokines (Th1-related IFN-γ, CXCL10/IP-10, CXCL9/MIG). TLR's active role in cytokine induction was supported by our ex vivo experiments, in which significant differences in response towards TLR ligands between influenza patients and controls (in IL-6, TNF-α, CXCL10/IP-10, IFN-α release), and changes in the 'responsiveness' during/after the illness (which was governed by the ligand used, cell type, disease stage, or immune exhaustion). A direct association between TLR hyperexpression and disease severity was not observed, but this was shown for the 'downstream' pro-inflammatory cytokines. Perpetuating, uncontrolled pro-inflammatory cytokine responses can lead to immunopathological damage in severe influenza, and further stimulation of TLRs at a more advanced disease stage may exacerbate tissue inflammation. It is uncertain whether TLR blockade alone can reduce inflammation as compensatory mechanisms might exist. Nevertheless, our data in natural influenza provided evidence that TLR's role in regulating the adaptive responses could be harnessed to boost immunogenicity of influenza vaccines (eg TLR9 or TLR7 ligands as adjuvants), which are already in clinical trials. This approach may be useful for vaccines for elderly and immunologically-naive people. Further study on the innate responses against influenza virus in infected patients is warranted.

Conclusion

Low TLR expression level is associated with a high viral load in vivo; TLR targeting and activation, using specific TLR agonists, can lead to rapid, broad-range protection against influenza challenges. Our data provide a basis for clinical studies on TLR targeting/activation, and assist their future planning. This novel strategy is useful for preventive intervention, such as pre-/post-exposure prophylaxis, which may contribute to influenza disease control.

Acknowledgement

This study was supported by the Research Fund for the Control of Infectious Diseases, Food and Health Bureau, Hong Kong SAR Government (#09080102). Results of this study have been published in: Lee N, Wong CK, Hui DS, et al. Role of human Toll-like receptors in naturally occurring influenza A infections. Influenza Other Respir Viruses 2013;7:666-75.

References

1. Arankalle VA, Lole KS, Arya RP, et al. Role of host immune response and viral load in the differential outcome of pandemic H1N1 (2009) influenza virus infection in Indian patients. PLoS One 2010;5:e13099.
2. Tuvim MJ, Gilbert BE, Dickey BF, Evans SE. Synergistic TLR2/6 and TLR9 activation protects mice against lethal influenza pneumonia. PLoS One 2012;7:e30596.
3. Lau YF, Tang LH, Ooi EE, Subbarao K. Activation of the innate immune system provides broad-spectrum protection against influenza A viruses with pandemic potential in mice. Virology 2010;406:80-7.
4. Wong JP, Christopher ME, Viswanathan S, et al. Activation of toll-like receptor signaling pathway for protection against influenza virus infection. Vaccine 2009;27:3481-3.

Effect of lifestyle factors on risk of mortality associated with influenza in elderly people

CM Wong *, WM Chan, L Yang, KP Chan, HK Lai, TQ Thach, LM Ho, TH Lam, JSM Peiris

KEY MESSAGES

1. Never-smokers had significantly lower risk of all-cause and cardiorespiratory mortality secondary to influenza than ex-smokers and current-smokers.
2. Regular and moderate exercisers had lower risk of all-cause and cardiorespiratory mortality secondary to influenza than those who had a sedentary lifestyle.
3. Consuming less alcohol was not associated with reduced mortality risk associated with influenza.
4. Community-dwelling older people in Hong Kong should be encouraged to maintain a healthy lifestyle in order to lower the mortality risk from influenza infection.

Hong Kong Med J 2014;20(Suppl 6):S16-9
RFCID project number: 09080532

[1] CM Wong *, [2] WM Chan, [1] L Yang, [1] KP Chan, [1] HK Lai, [1] TQ Thach, [1] LM Ho, [1] TH Lam, [3] JSM Peiris

[1] *School of Public Health, Li Ka Shing Faculty of Medicine, The University of Hong Kong*
[2] *Department of Health, The Government of the Hong Kong Special Administrative Region*
[3] *Department of Microbiology, Li Ka Shing Faculty of Medicine, The University of Hong Kong*

* Principal applicant and corresponding author: hrmrwcm@hku.hk

Introduction

Influenza poses a major health hazard in terms of mortality and morbidity, particularly in elderly people. It is controversial whether vaccination can effectively reduce the incidence of influenza infection and the risk of hospitalisation and mortality in elderly people.[1] The time delay with respect to vaccine production results in an occasional mismatch between vaccines and circulating strains of influenza. Annual vaccination campaigns are also hampered by concerns over potential adverse events of vaccines.[2] Therefore, preventive approaches such as improving personal hygiene and maintaining a healthy lifestyle should be encouraged.

Effects of smoking, drinking alcohol, and physical exercise on infection risks of influenza have been studied. This study assessed the modification effects of smoking, exercise, and alcohol consumption on the mortality risk from influenza in a large elderly cohort with a follow-up period of nearly 12 years.

Methods

This study was conducted from September 2009 to August 2010. From May 1998 to December 2001, 66 820 older people (aged ≥65 years) living in the community were recruited from 18 elderly health centres (EHCs) managed by the Department of Health. Data on the participants' lifestyle (history of smoking, exercise frequency, and alcohol consumption) and socioeconomic status (housing type, education, and monthly expenditure) were collected by trained nurses and doctors using a standardised questionnaire. The participants' health status was assessed using comprehensive clinical examination, and any chronic conditions were recorded at the first visit.

Smoking status was categorised as never-, current-, and ex-smokers, where ex-smokers were those who had ever smoked but had stopped for ≥1 year. Alcohol consumption status was categorised as never-, ex-, and social/regular drinkers, where never drinkers were those who had never drunk alcohol, ex-drinkers were those who had drunk alcohol previously, and social and regular drinkers were those who drank alcohol on <4 and ≥4 days per week, respectively. Exercise was categorised as sedentary, moderate-, and frequent-exercise based on the self-reported frequency and duration of regular exercise, where sedentary was defined as not doing any exercise at all, moderate exercise was defined as not doing exercise every day or for <30 minutes each time, and frequent exercise was defined as doing exercise for >30 minutes every day.

The death registration data were linked to the cohort baseline using the Hong Kong identity card number. Participants with an unknown date of death (n=194) were excluded, and the final sample included 66 626 elderly people. All participants with unknown vital status were censored on 2 January 2010, and those who died from accidents were censored on the reporting dates of death in their death registration records. Influenza and respiratory syncytial virus (RSV) virology data were obtained from the microbiology laboratory of Queen Mary Hospital. The weekly proportions of specimens

positive for influenza (or RSV) were used as a proxy for influenza (or RSV) virus activity. Meteorology data of temperature and relative humidity were obtained from the Hong Kong Observatory.

Statistical analysis

Time-dependent Cox proportional hazards models were used to estimate the hazard ratio of influenza-associated mortality for all-cause and chronic respiratory disease (CRD) mortality. To adjust for confounding seasonal factors, time-dependent variables for long-term and seasonal trends of mortality, meteorological factors, weekly average concentrations of ambient air pollutants, and co-circulation of RSV were included in the models with 'week' as the unit of time. Age, sex, education, housing type, co-morbidity score, smoking, exercise, and alcohol consumption were added into the models as time-independent variables. Effect modification of smoking, alcohol consumption, and exercise was assessed by the interaction terms of influenza virus activity and dummy variables for each lifestyle factor in the interaction models. The statistical significance of interaction terms was assessed by likelihood ratio tests between models with and without interaction terms. Stratified analyses were also conducted for each stratum of smoking, alcohol consumption, and exercise no matter whether their interaction terms were significant in the interaction models. Influenza-associated excess risk of mortality for each stratum of lifestyle factors was measured by the percentage change in the hazard associated with every 10% increase of influenza virus activity. A P value of <0.05 was considered statistically significant.

Results

The interaction between influenza virus activity and each of the three lifestyle habits in terms of all-cause

TABLE. Difference in excess mortality risks (in %) associated with 10% increase in influenza virus activity relative to the reference groups

Parameter	Per 10% increase in influenza activity					
	Both sexes	P value*	Men	P value*	Women	P value*
All-cause mortality						
Smoking						
Never	0	0.657	0	0.643	0	0.126
Ex	2.1 (-2.5 to 6.9)		2.2 (-4.8 to 9.7)		3.4 (-4.6 to 12.1)	
Current	1.4 (-4.4 to 7.5)		-1.2 (-9.0 to 7.3)		11.3 (0.0 to 23.8)	
Alcohol consumption						
Never	0	0.619	0	0.735	0	0.812
Ex	1.8 (-3.8 to 7.7)		2.2 (-5.0 to 10.1)		2.8 (-7.3 to 14.0)	
Social/regular	-1.8 (-7.1 to 3.9)		-1.1 (-8.0 to 6.4)		-1.8 (-11.5 to 9.1)	
Exercise						
Sedentary	0	0.139	0	0.167	0	0.180
Moderate	-3.0 (-8.5 to 2.8)		-7.7 (-15.3 to 0.6)		0.7 (-7.0 to 9.1)	
Frequent	-5.4 (-10.6 to 0.1)		-6.4 (-13.7 to 1.5)		-4.4 (-11.6 to 3.3)	
Chronic respiratory disease mortality						
Smoking						
Never	0	0.751	0	0.393	0	0.051
Ex	-1.7 (-7.8 to 4.9)		-5.5 (-14.5 to 4.3)		1.1 (-9.6 to 13.1)	
Current	1.9 (-6.6 to 11.1)		-7.4 (-18.0 to 4.5)		21.1 (4.2 to 40.8)	
Alcohol consumption						
Never	0	0.020	0	0.174	0	0.056
Ex	5.4 (-2.4 to 13.8)		2.9 (-6.9 to 13.8)		13.0 (-1.8 to 29.9)	
Social/regular	-9.1 (-16.6 to -0.9)		-7.8 (-17.3 to 2.8)		-12.7 (-26.3 to 3.6)	
Exercise						
Sedentary	0	0.046	0	0.120	0	0.131
Moderate	4.0 (-4.4 to 13.0)		-2.1 (-13.3 to 10.6)		9.6 (-2.3 to 23.1)	
Frequent	-4.0 (-11.6 to 4.3)		-9.8 (-19.8 to 1.5)		(-9.4 to 14.1)	

* Likelihood ratio tests for interaction between influenza and lifestyle factors on the mortality effects

and CRD mortality was analysed. Smoking was marginally significantly associated with all-cause mortality in women (P=0.051), whereas alcohol consumption (P=0.020), and exercise (P=0.046) were significantly associated with CRD mortality in both sexes combined (Table).

For every 10% increase in influenza virus activity in the community, the risk of CRD mortality increased by 25.8% (P<0.05) in female current smokers, which was more than 10-fold higher than that of female never- and ex-smokers. Results were similar for all-cause mortality in female current smokers with a smaller increase in mortality risk of 16.3%. However, the excess risk of mortality was not significant among the three male smoking subgroups, but male ex-smokers tended to have a higher mortality risk attributable to influenza than never-smokers. For both sexes combined, ex-smokers had a similar excess risk of influenza-associated CRD mortality as current smokers (Fig). Both female and male ex-alcohol drinkers had significantly higher excess risk of all-cause and CRD mortalities associated with influenza, but the excess risk of mortality was significant only in the male and combined sex groups. Never drinkers and social/regular drinkers had similar excess risk of all-cause mortality, and none of their estimates were significant (Fig). The excess risk of mortality

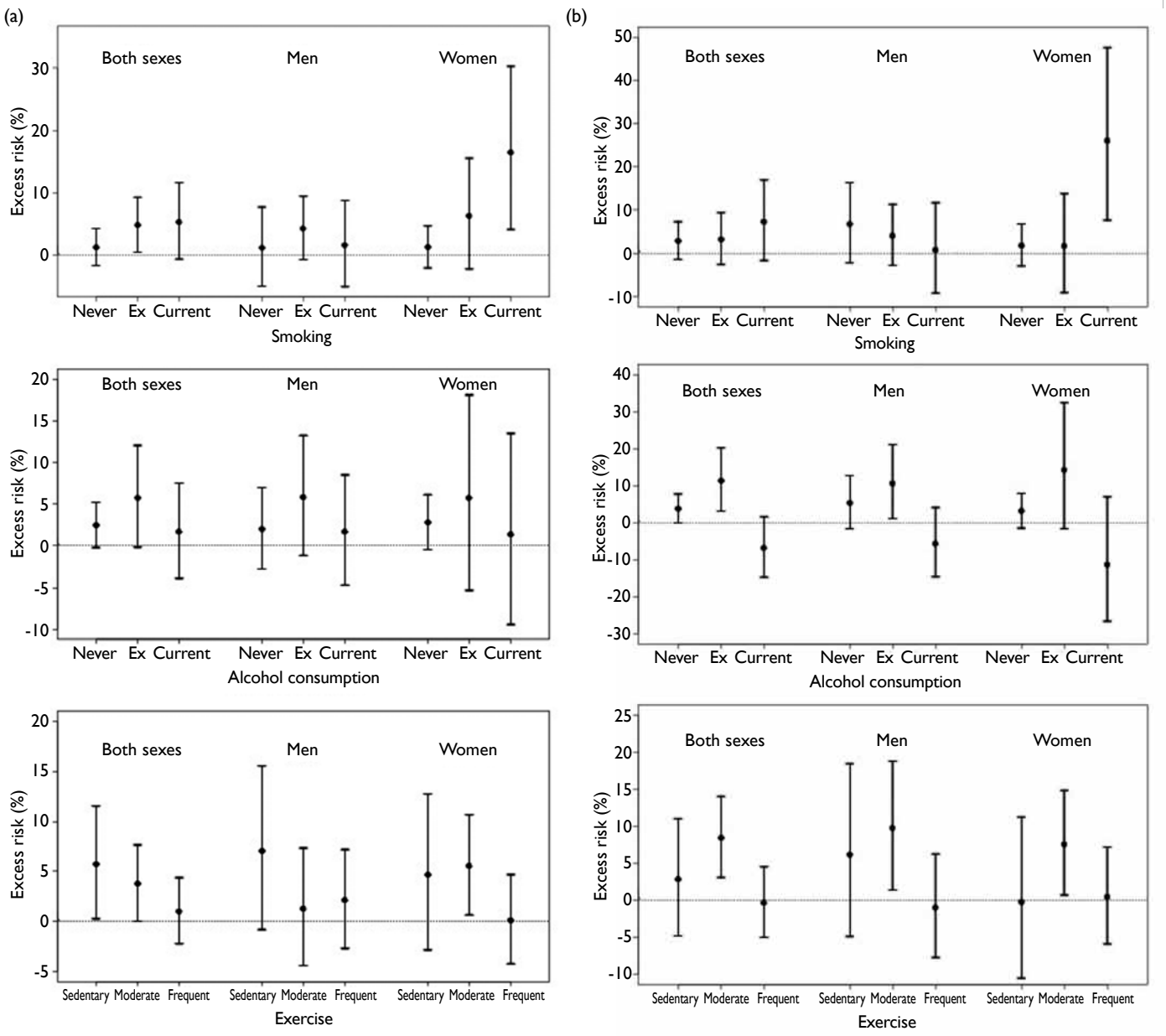

FIG. Excess mortality risks (in %) associated with 10% increase in influenza virus activity, stratified by the sex and lifestyle groups: (a) all-cause mortality and (b) chronic respiratory disease mortality

associated with influenza was lower for frequent exercisers than for the other two groups, with the exceptions of all-cause mortality in men and CRD mortality in women. Participants who took moderate exercise had lower influenza-associated excess risk of all-cause mortality than those who had a sedentary lifestyle for the men and combined sex groups, but had consistently higher excess risk of CRD mortality among both men and women (Fig).

Discussion

Mortality risks associated with influenza were much higher for current smokers than for those who had never smoked among both female and male older people. Smoking can cause structural changes in respiratory epithelial cells and suppress both cell- and humoral-mediated immunity responses against infections.[3]

Regular moderate exercise is associated with reduced viral load and increased serum level of inflammatory factors in mice infected with influenza viruses, but the association between exercise and respiratory infections has not been established.[4] Our study provides further evidence for a potential beneficial effect of occasional and frequent exercise in lowering the mortality risks of influenza infection among older people. Although the intensity of exercise taken by each participant in the moderate and frequent exercise groups was unknown, the type of exercise suggested that nearly 90% were exercising normally at low to moderate intensity such as stretching, slow walking on level ground, and Tai Chi. Further studies using a standardised exercise protocol combined with accurate measurement for energy expenditure and laboratory tests for respiratory pathogens are warranted.

Chronic exposure to ethanol increases the susceptibility of mice to infection from respiratory viruses by suppressing the cellular response and altering the immune cytokine levels.[5] However, in our study, excess risks for CRD and all-cause mortality attributable to influenza were lower among the social/regular drinkers than among the ex-drinkers and never drinkers. A protective effect (despite not being significant) was observed for social/regular drinkers for CRD mortality. In these participants, only 456 (2%) men had ≥3 drinks per day and 64 (0.1%) women had ≥2 drinks per day. Therefore, it seems that few of the EHC members were heavy drinkers, which could explain why we did not observe an adverse effect of alcohol consumption for mortality risk associated with influenza. Furthermore, we did not consider the heterogeneous effects of the different types of alcoholic drinks due to lack of such data.

There were limitations to our study. First, the vaccination history of each participant was not known, which could bias the estimates of influenza effects. Second, estimates for influenza effects were based on modelling the association between influenza activity and incidence of death, ie whether death rates increased along with increased influenza virus activity. However, it would be unrealistic to make a laboratory diagnosis for each suspected influenza case given the cost of laboratory tests. Third, the participants were recruited through their voluntary visits to the EHC, therefore they tend to be healthier and more health conscious than those dwelling in the community but never visited an EHC. Nevertheless, the small Cohen's effect sizes show that our cohort is representative in lifestyle and socioeconomic aspects. Last, all the lifestyle data were collected at baseline during the participants' first visit to the EHC. Misclassification bias could have been introduced if some participants had changed their habits during the follow-up period.

Conclusion

Never-smokers had a lower mortality risk attributable to influenza than ex- and current-smokers. Frequent exercisers also had a lower risk than sedentary people. However, the beneficial effects of consuming less alcohol were not conclusive. Taken together, maintaining a healthy lifestyle is associated with significant reduction of the mortality risks attributable to influenza.

Acknowledgements

This study was supported by the Research Fund for the Control of Infectious Diseases, Food and Health Bureau, Hong Kong SAR Government (#09080532); and the Area of Excellence Scheme of the University Grants Committee, Hong Kong SAR Government (AoE/M-12/06). We thank the staff of the Elderly Health Centres for their assistance in data collection and entry.

References

1. Simonsen L, Taylor RJ, Viboud C, Miller MA, Jackson LA. Mortality benefits of influenza vaccination in elderly people: an ongoing controversy. Lancet Infect Dis 2007;7:658-66.
2. Iskander J, Broder K. Monitoring the safety of annual and pandemic influenza vaccines: lessons from the US experience. Expert Rev Vaccines 2008;7:75-82.
3. Arcavi L, Benowitz NL. Cigarette smoking and infection. Arch Intern Med 2004;164:2206-16.
4. Martin SA, Pence BD, Woods JA. Exercise and respiratory tract viral infections. Exerc Sport Sci Rev 2009;37:157-64.
5. Crews FT, Bechara R, Brown LA, et al. Cytokines and alcohol. Alcohol Clin Exp Res 2006;30:720-30.

Role for autophagy in cellular response to influenza virus infection

AHY Law, DCW Lee, TYY Leon, ASY Lau *

KEY MESSAGES

1. A differential induction of autophagy was noted between influenza virus A/Hong Kong/54/98 (H1N1) and A/Quail/Hong Kong/G1/97 (H9N2/G1) infections.
2. The H9N2/G1 virus, which shows a delay in apoptosis activation, induces autophagy to a greater extent than the H1N1 virus.
3. Autophagy is not involved in H9N2/G1 virus replication in primary human blood macrophages.
4. Using 3-methyladenine to inhibit autophagy and small interfering RNA to silence the autophagy gene (Atg5), autophagic responses play a role in influenza virus-induced CXCL10 and interferon-α expression in human macrophages.

Hong Kong Med J 2014;20(Suppl 6):S20-4
RFCID project number: 09080832

AHY Law, DCW Lee, TYY Leon, ASY Lau

Cytokine Biology Group, Department of Paediatrics and Adolescent Medicine, Li Ka Shing Faculty of Medicine, The University of Hong Kong

* Principal applicant and corresponding author: paedoff@hku.hk

Introduction

The outbreak of avian influenza A (H5N1/97) virus infection in Hong Kong is the first documented case of direct transmission of the H5N1 virus from birds to humans. The high mortality rate of >60% caused great concern to the public and government. In addition, avian influenza H9N2 viruses have become highly prevalent in poultry in many countries and have caused human infections. The high prevalence, wide geographic range, rapid evolution, and frequent reassortment of H9N2 viruses in poultry,[1] combined with the increasing number of avian influenza infections in humans, highlights their pandemic and zoonotic potential.

Apoptosis and autophagy constitute the two processes through which superfluous, damaged, or aged cells or organelles are eliminated.[2] Apoptosis has been shown to be one of the most effective host defence mechanisms against microbial pathogens. The cell death process results in inhibition of virus replication, limitation of virus dissemination, and minimisation of uncontrolled inflammatory responses. Avian influenza (H5N1/97) and its precursors trigger a caspase-dependent but delayed apoptotic response in human macrophages, compared with human influenza viruses (H1N1 and H3N2).[3]

Autophagy is a tightly regulated cellular homeostatic process involving the sequestration of parts of the cytosol and intracellular organelles within double-membraned autophagic vacuoles that are delivered to lysosomes for degradation. Autophagy plays essential roles in physiological processes such as cellular responses to starvation, cell survival, and death. Additionally, autophagy has been implicated in cancer, neurodegeneration, and myopathies, and it is involved in both innate and acquired immunity.[4] Autophagy is involved in the host defence mechanism against pathogens, including bacteria and viruses.[5] The antiviral role of autophagy is strengthened by the involvement of the autophagic process in the induction of interferon (IFN) in virus infection.[5]

To investigate the mechanisms underlying the diversion of cell death processes, we hypothesised that avian influenza viruses divert the cell death pathways from apoptosis, which ultimately involves whole cell death and degradation of cellular organelles, to that of autophagy, which is a self-sustained process resulting in removal of unwanted subcellular structures leading to prolonged survival of the avian virus-infected cells. With longer survival of virus-infected cells resulting from autophagy activation, there are opportunities for completion of virus replication and consequent immune dysregulation.

Methods

This study was conducted from October 2009 to September 2011. Human blood macrophages from healthy donors (Hong Kong Red Cross Blood Transfusion Service) were prepared as described previously.[3] Differentiated macrophages were obtained after culturing for 14 days. Influenza viruses A/Quail/Hong Kong/G1/97 (H9N2/G1) and A/Hong Kong/54/98 (H1N1) were grown in Madin-Darby canine kidney (MDCK) cells and were purified by pre-adsorption to and elution from turkey red

blood cells. Virus infectivity was determined by titration on MDCK cells.

Cells were infected with the viruses at a multiplicity of infection (MOI) of two or at the indicated dose for 30 minutes at 37°C. The supernatant containing the virus inoculum was then removed, and the cells were incubated in serum-free medium supplemented with 0.6 μg/mL penicillin and 60 μg/mL streptomycin. The mock-treated control was incubated with the buffer under parallel conditions.

To measure intracellular protein expression, whole-cell lysates were prepared by using total lysis buffer (50 mM Tris-hydrochloride, pH 7.4, 150 mM sodium chloride, 50 mM sodium fluoride, 10 mM β-glycerophosphate, 0.1 mM ethylene diamine tetraacetic acid, 10% glycerol, 1% Triton X-100) containing a protease inhibitor cocktail. For western blot analysis, 30 μg of protein was heat-denatured and separated by 10% sodium dodecyl sulphate-polyacrylamide gel electrophoresis, and transferred onto a nitrocellulose membrane for assaying protein levels by using enhanced chemiluminescence solution.

For the detection of autophagosome formation, cells were fixed with 4% paraformaldehyde and permeabilised with 0.25% Triton X-100 for 5 minutes. The cells were stained with antibodies specific to LC3B and rhodamine-conjugated anti-rabbit secondary antibodies. Nuclei were counterstained with 4,6-diamidine-2-phenylindole dihydrochloride, and the immunocytochemical staining was examined under fluorescence microscopes.

The production of chemokines and interferons upon influenza infection were assayed by TaqMan Gene Expression Assays (Applied Biosystems; Life Technologies, Carlsbad, CA, USA) and enzyme-linked immunosorbent assays (R&D Systems, Minneapolis, MN, USA).

In studying the involvement of autophagy in virus replication and cytokine production, expression of Atg5 in human blood macrophages was knocked down by short interfering RNA (siRNA) oligos specific to Atg5 (siAtg5). Non-targeting siRNA oligos (siCtrl) were used as controls. Macrophages were transfected with either the siAtg5 or siCtrl at indicated concentrations using jetPEI transfection reagent (Polyplus-transfection, Illkirch, France). At 48 hours after transfection, cells were infected with the viruses, and then cells were harvested at indicated time points for further analyses.

Results

H9N2/G1 is a stronger autophagy inducer than H1N1

To investigate whether influenza virus can induce autophagy, differentiated primary human blood

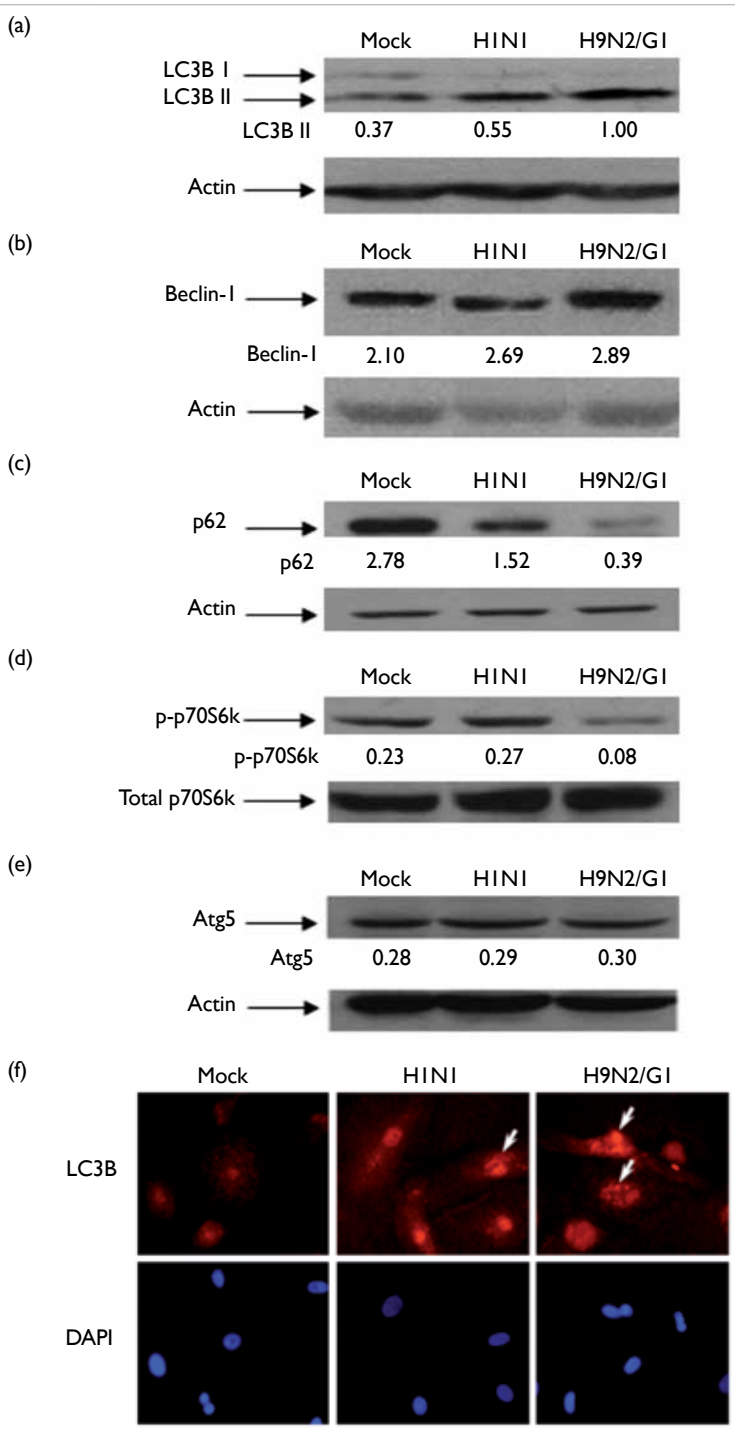

FIG 1. Autophagy is induced by H1N1 and H9N2/G1 influenza viruses. Human blood macrophages are mock-infected or infected with H1N1 or H9N2/G1. Whole-cell lysates are harvested and expressions are examined by western blot analysis. Actin is used as a loading control. (a) LC3B, (b) Beclin-1, (c) p62, (d) phosphorylation levels of p70S6K (Thr389), and (e) Atg5 are examined. Total p70S6K is used as a loading control. The band intensities of the indicated proteins are measured and then normalised to those of the corresponding actin. The normalised values are presented. Representative figures of experiments from three independent blood donors are shown. (f) Autophagosomes are examined by staining the mock-, H1N1-, or H9N2/G1-infected cells with antibodies specific to LC3B. DAPI is used to stain the nuclei. Arrows indicate LC3B-positive vesicles (x3400). (Figures were adapted with permission from: Law AH, Lee DC, Yuen KY, Peiris M, Lau AS. Cellular response to influenza virus infection: a potential role for autophagy in CXCL10 and interferon-alpha induction. Cell Mol Immunol 2010;7:263-70.)

macrophages (PBMacs) were infected with avian influenza virus H9N2/G1 or seasonal H1N1 virus at MOI of two. Expressions of key autophagy genes were investigated. At 19 hours post-infection, whole-cell lysates were prepared and conversion of LC3B I to II, a hallmark of autophagy, was analysed by western blot using antibodies specific to LC3B. Actin was used as a loading control. LC3BI was converted to LC3B II at a higher efficiency in cells infected with H9N2/G1 virus than with H1N1 virus (Fig 1a). Consistent with the conversion of LC3B, the expression level of Beclin-1, another autophagic marker, was also increased in cells infected with H9N2/G1 compared with H1N1 (Fig 1b). In addition, the level of p62 protein, a polyubiquitin-binding protein was also examined. The p62 protein can bind directly to LC3 proteins that enhance the degradation of ubiquitinated proteins in the lysosome through the autophagic processes. The p62 protein can also be degraded by autophagy. Its expression level, therefore, indicates the autophagic status of the cell. The p62 expression decreased by approximately 45% in macrophages with H1N1 infection when compared with mock-treated cells, whereas the level was decreased by about 84% in H9N2/G1-infected cells (Fig 1c). Furthermore, autophagy was negatively regulated by mTOR. Inhibition of mTOR led to induction of autophagy. As p70S6K is a direct target of mTOR, the phosphorylation of p70S6K at threonine 389 was examined to determine the activity of the rapamycin-sensitive mTOR complex. Phosphorylation of p70S6K at threonine 389 in H9N2/G1-infected macrophages decreased at 2 hours post-infection when compared with mock-treated cells (Fig 1d), whereas there was no significant change in H1N1-infected cells. In contrast, the expression level of Atg5, another autophagy-related protein involving in autophagosome formation, was not affected by the influenza virus infections (Fig 1e).

Autophagosomes were also examined by immunocytochemistry at 19 hours post-infection (Fig 1f). Consistent with the western blots, LC3B-positive vesicles with a punctate-staining pattern were found in cells infected with H9N2/G1 or H1N1. Moreover, more prominent staining was found in cells infected with H9N2/G1 when compared with those infected with H1N1. The H9N2/G1 virus induced more autophagic responses than H1N1.

Autophagy is not involved in influenza virus replication in macrophages

Association between concomitant activation of autophagy and significant enhancement of influenza virus replication was investigated. We treated the PBMacs with rapamycin, which is a well-known autophagy inducer through inhibition of mTOR, and then infected the cells with H1N1 virus. Cell culture supernatant was harvested at 48 hours post-infection for viral titre determination. Treatment with rapamycin did not significantly change the virus titres (Fig 2a).

The effect of inhibiting the virus-induced autophagy on virus replication was also investigated. We pre-treated the PBMacs with a chemical inhibitor, 3-methyladenine (3-MA), which inhibits autophagy by suppressing class III phosphatidylinositol-3-

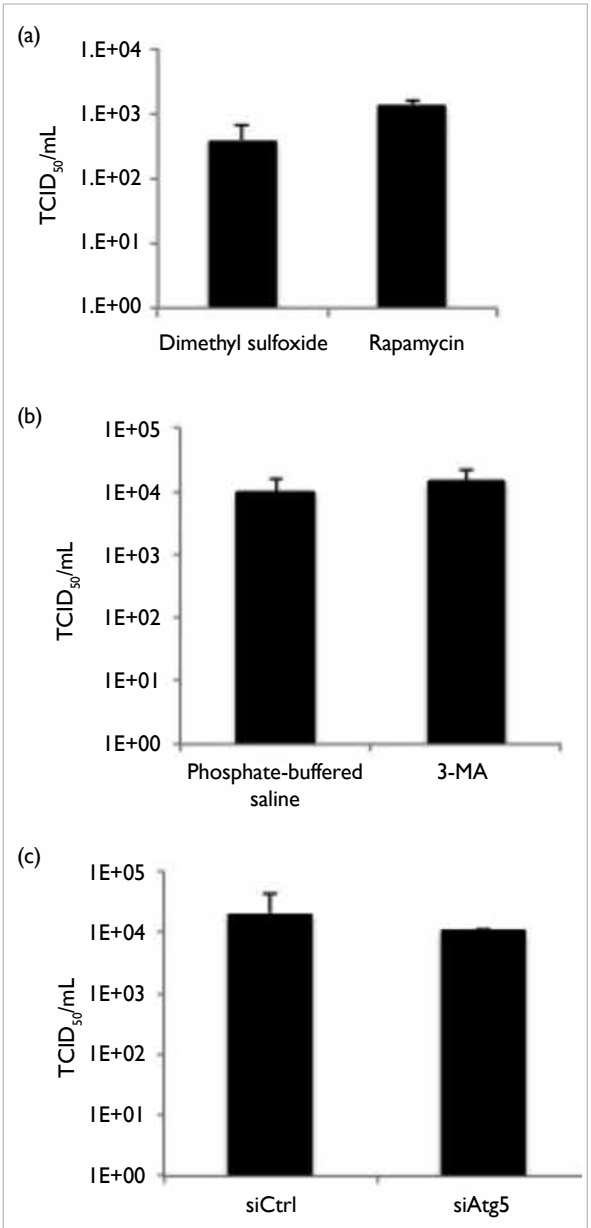

FIG 2. Autophagy is not involved in influenza virus replication. (a) Macrophages are pre-treated with 10 nM of rapamycin for 1 hour and then infected with H1N1 at multiplicity of infection of two. (b) Macrophages are pre-treated with 10 mM of 3-methyladenine (3-MA) for 1 hour or (c) transfected with the Atg5-specific siRNA oligos (siAtg5) or the control oligos (siCtrl) at 48 hours before infection. Cells are then infected with H9N2/G1 virus at MOI of two. At 48 hours post-infection, culture supernatants are collected. The virus titres are calculated using $TCID_{50}$ assay.

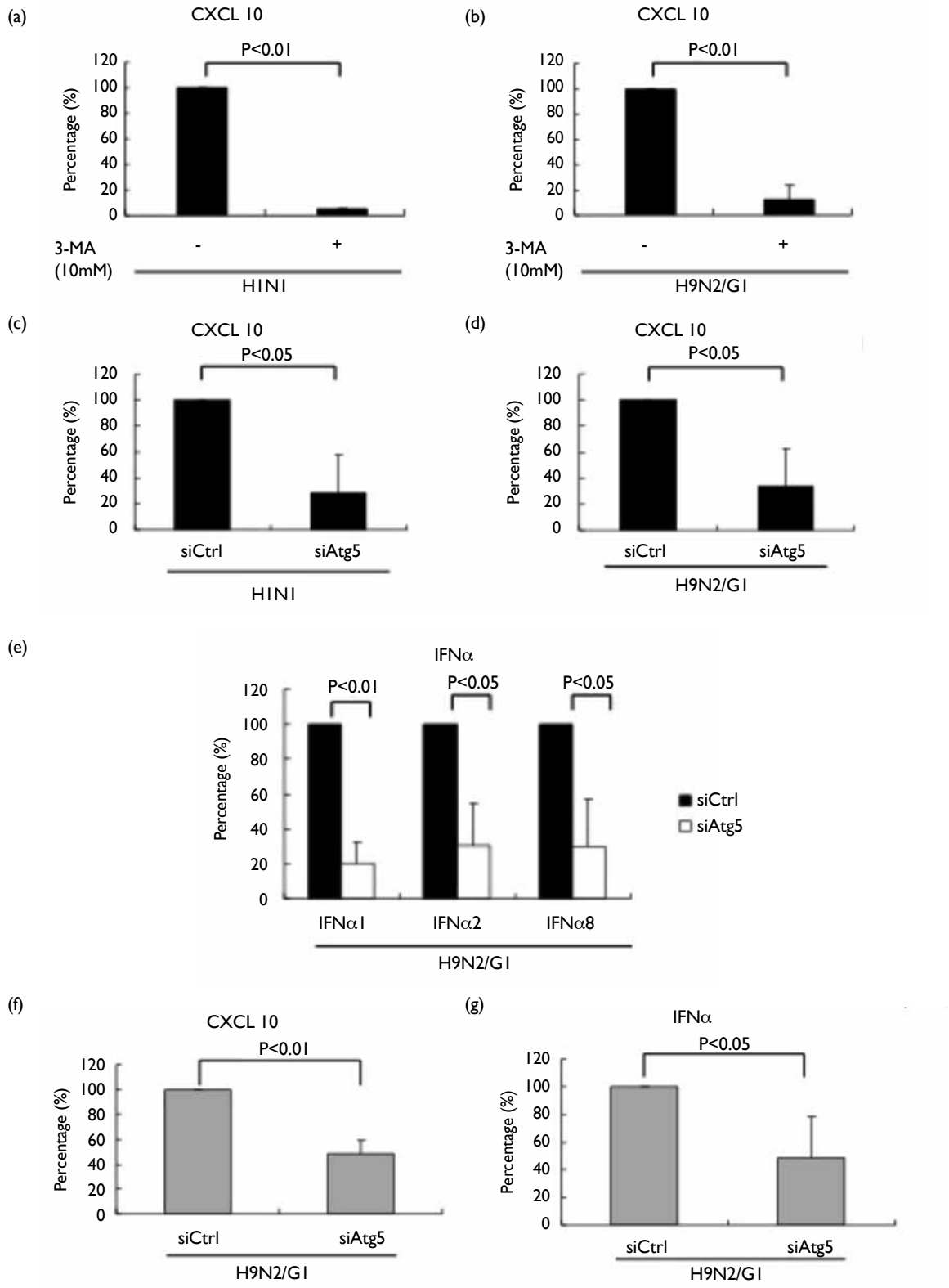

FIG 3. Inhibition of autophagy suppresses influenza-induced CXCL10 and IFN-α expression. Macrophages are pre-treated with 10 mM of 3-methyladenine (3-MA) before infection or transfected with siAtg5 or siCtrl at 200 nM. Cells are then infected with (a, c) H1N1 or (b, d) H9N2/G1. The relative CXCL10 mRNA levels are examined at 3 hours post-infection by TaqMan Gene Expression Assay, as are (e) relative mRNA levels of IFN-α1, -α2, and -α8 in siRNA-transfected cells with H9N2/G1 infections. Macrophages are transfected with siAtg5 or siCtrl at 200 nM. At 48 hour post-transfection, cells are infected with H9N2/G1. Quantities of (f) CXCL10 and (g) IFN-α in the culture supernatants at 8 hours post-infection are measured by enzyme-linked immunosorbent assay. (Figures were adapted with permission from: Law AH, Lee DC, Yuen KY, Peiris M, Lau AS. Cellular response to influenza virus infection: a potential role for autophagy in CXCL10 and interferon-alpha induction. Cell Mol Immunol 2010;7:263-70.)

kinase. Cells were then infected with H9N2/G1 virus and the virus titres were measured at 48 hours post-infection. No significant difference was found in the viral titre after the 3-MA treatment (Fig 2b). In addition to the chemical inhibitor, the effects of enhanced activation of autophagy in H9N2/G1 virus replication were further investigated by inhibiting the autophagic pathway using the siRNA silencing method. At 48 hours after transfecting the PBMacs with Atg5-specific siRNA oligos or control oligos, the cells were infected with H9N2/G1 virus at MOI of two and viral loads in the cell culture supernatant were measured by $TCID_{50}$ assay at 48 hours post-infection. No significant difference was found in the cells transfected with the Atg5-specific oligos and the control oligos (Fig 2c). Therefore, with the inhibition of the autophagic pathway by 3-MA or Atg5-specific siRNA oligos, autophagy did not involve H9N2/G1 replication in PBMacs.

Autophagic responses play a role in influenza virus-induced CXCL10 and IFN-α expressions

Whether autophagy was involved in the hyperinduction of chemokine and IFN was examined. The autophagic pathway 3-MA was blocked, or the PBMacs were transfected with siRNA oligos specific to Atg5. With the 3-MA pre-treatment, mRNA levels of CXCL10 induced by H1N1 or H9N2/G1 were reduced significantly as determined by TaqMan Gene Expression Assays (Figs 3a-b). At 48 hours post-transfection of the siRNA oligos, the cells were infected with H1N1 and H9N2/G1. Total RNA was collected at 3 hours post-infection, and the mRNA level of CXCL10 was measured by TaqMan Gene Expression Assays. The mRNA levels of CXCL10 induced by the two viruses were significantly reduced upon knockdown of Atg5 (Figs 3c-d). In siAtg5-transfected cells at 3 hours post-infection, CXCL10 mRNA levels were decreased by 72% and 67% in H1N1- and H9N2/G1-infected cells, respectively, when compared with those transfected with siCtrl. The mRNA levels of IFN-α1, -α2, and -α8 were measured in H9N2/G1-infected cells by TaqMan Gene Expression Assays. Similarly, in cells transfected with siAtg5, the IFN-α1, -α2, and -α8 mRNA levels were significantly decreased by around 70% (Fig 3e). The CXCL10 and IFN-α protein levels in culture supernatants of Atg5 knockdown cells were measured. At 8 hours post-infection with H9N2/G1, the level of CXCL10 in cell culture supernatants was decreased by about 50% (Fig 3f), concomitant with reduced Atg5 expression. Similarly, IFN-α expression was decreased by approximately 50% in cells transfected with siAtg5 (Fig 3g).

Conclusion

In human macrophages, autophagy played a role in H1N1- and H9N2/G1-induced CXCL10 and IFN-α production but not in virus replication. Our results may provide new insights into the underlying mechanisms of the pathogenesis of avian influenza virus infections.

Acknowledgement

This study was supported by the Research Fund for the Control of Infectious Diseases, Food and Health Bureau, Hong Kong SAR Government (#09080832).

References

1. Xu KM, Smith GJ, Bahl J, et al. The genesis and evolution of H9N2 influenza viruses in poultry from southern China, 2000 to 2005. J Virol 2007;81:10389-401.
2. Maiuri MC, Zalckvar E, Kimchi A, Kroemer G. Self-eating and self-killing: crosstalk between autophagy and apoptosis. Nat Rev Mol Cell Biol 2007;8:741-52.
3. Mok CK, Lee DC, Cheung CY, Peiris M, Lau AS. Differential onset of apoptosis in influenza A virus H5N1- and H1N1-infected human blood macrophages. J Gen Virol 2007;88:1275-80.
4. Mizushima N, Komatsu M. Autophagy: renovation of cells and tissues. Cell 2011;147:728-41.
5. Schmid D, Munz C. Innate and adaptive immunity through autophagy. Immunity 2007;27:11-21.

Hepatitis B virus array for genotyping and mutation detection

V Chan *, CL Lai, KM Chan, MF Yuen

KEY MESSAGES

1. A comprehensive hepatitis B virus (HBV) array providing simultaneous analysis of HBV genotypes, mutations of reverse-transcriptase polymerase gene and mutations of S gene was developed.
2. The specificity and sensitivity of the HBV array was validated through analysis of 506 serum samples.
3. The array demonstrated improved sensitivity compared with existing commercial kits, with a detection limit down to ~28 copies/mL of HBV. It also enabled early detection of emergence of drug-resistant mutants.
4. The array may be useful for clinicians in making timely decisions on switching to alternative drugs.

Hong Kong Med J 2014;20(Suppl 6):S25-7
RFCID project number: 06060572

V Chan, CL Lai, KM Chan, MF Yuen

Department of Medicine, Queen Mary Hospital

* Principal applicant and corresponding author: vnychana@hku.hk

Introduction

Hepatitis B virus (HBV) infection is a serious global health problem affecting about 2 billion people worldwide, of whom 350 million are chronic HBV carriers. The HBV is the tenth leading cause of death, with about one million deaths annually secondary to chronic hepatitis, cirrhosis, or hepatocellular carcinoma (HCC).[1] The HBV is virtually endemic throughout Asia and Africa, and most chronic HBV infections are acquired perinatally or during childhood. For individuals with HBV infection, antiviral treatment is an effective way to reduce morbidity and mortality, and life-long antiviral therapy is advocated.[2] However, in some patients, resistant viral strains carrying mutations in the B, C, and D domains of the HBV reverse transcriptase (rt) polymerase gene may emerge with prolonged therapy.[3] These patients then have a higher risk of developing HCC than patients without resistant virus. Close monitoring of serum for early detection of any drug-resistant mutant is important to enable timely switching to or adding of other antiviral drugs to achieve adequate viral suppression.

For patients who have undergone liver transplantation for hepatitis B–related end-stage liver disease, prophylaxis against recurrent HBV infection is given by administration of hepatitis B immunoglobulins derived from vaccinated subjects. The emergence of immune escape HBV mutants results in viral persistence despite adequate antibody titres. Identification of such S gene mutations helps devise alternative vaccines or post-transplant prophylaxis.[4] Different genotypes of HBV may predispose to disease complications (such as cirrhosis or HCC) and response to treatment.

Kits for the separate determination of viral mutants and genotypes are commercially available. The design of a comprehensive array to enable simultaneous detection of rt polymerase gene mutations, S gene mutations, and genotypes is useful.

Methods

This study was conducted from November 2006 to October 2008. Oligonucleotide primers pertaining to both the wild type and mutant sequences at the various positions along the rt polymerase and S genes of HBV were spotted onto coated glass slides. Each slide contained two sections of oligonucleotides for analysis of two different test samples. In addition, in each section, the oligonucleotides were spotted six times. Oligonucleotides for the detection of the eight genotypes of HBV were also spotted. Asymmetric polymerase chain reaction (PCR) product of the HBV gene fragment was prepared from a patient's serum DNA and used in an allele-specific arrayed primer extension reaction (AS-APEX) on the spotted array as described previously.[5]

Serum DNA from 100 unrelated HBV patients was analysed. The results were compared with those assayed previously using a commercial kit (Inno-Lipa HBV Genotyping assay; Innogenetics, Ghent, Belgium). Samples with discordant results were sequenced to ascertain the correct mutation.

Sensitivity and specificity of the array were confirmed by analysing serial samples from 45 HBV patients on long-term follow-up at the hepatology clinic of the Queen Mary Hospital. Typically serum samples were collected pre-treatment and five to seven times during therapy over a period of

TABLE. Longitudinal follow-up study of patients receiving antiviral therapy

Patient no: drug (date taken)	Initial	I	II
Patient 1: lamivudine (97), LG (04)	AA67 (11/8/97) (A67)	AA68 (20/5/04)*	AA69 (9/6/04)
Results using commercial kit	424.5 x10^6 c/mL (lamivudine↓, LG ↓)	3.74 x10^6 c/mL (180M, 204V)	3.44 x10^5 c/mL (80I, 80V, 180M, 204I)
Results of both genotype, and mutants detected by the array	C: wild type only	C: L80, 80I, 80V, V84, 84M, L180, 180M, 204I	C: L80, 80I, 80V, V84, 84M, L180, 180M, 204I
Patient 2: lamivudine, LG	AA83 (3/9/97)	AA84 (8/9/04)*	AA86 (12/10/04)
Results using commercial kit	311.3 x10^6 c/mL (Lamivudine↓ LG↓)	28.1 x10^6 c/mL (180M, 204I)	1.63 x10^6 c/mL (80I, 80V, 180M, 204I)
Results of both genotype, and mutants detected by the array	C: wild type only	C: 80I, 80V, L82, 82M, L180, 180M, 204I	C: 80I, 80V, L180, 180M, 204I
Patient 3: adefovir (15/11/03)	50 (13/1/04)*	M1 (14/6/04)	M2 (21/9/04)
Results using commercial kit	8.26 x10^5 c/mL (80I, 180M)	1.2 x10^3 c/mL (80I, 180M, L180, 204I)	1.65 x10^2 c/mL
Results of both genotype, and mutants detected by the array	B, C: S78, T78; 80I, S85, 85A, L179, 179P, 180M, V191, 191I, 204I	B: 80I, 180M, 204I	B: L82, 82M, T128, 128A, V207, 207M
Patient 4	37 (26/4/04)	N1 (3/1/05)*	N2 (5/12/05)
Results using commercial kit	7.9 x10^4 c/mL (80V, 80I)	<2000 c/mL (no polymerase chain reaction product) [10/10/05 11935 c/mL 80I]	1.6 x10^3 c/mL
Results of both genotype, and mutants detected by the array	C: L80, 80I, 128A, L180, 180M, 229V (S gene)	C: 80I, 128A, 204I	C: 80I, 128A, 204I

* Earlier detection of mutants by hepatitis B virus array

1 to 3 years. The results of the array analysis were compared with those detected with the Inno-Lipa kit. Genotypes of these samples were also recorded.

Quantitative PCR based on the TaqMan Technology was used to assess the copy number of HBV mutants in five different HBV serum samples. Each serum sample was then subjected to a serial doubling dilution with the same starting copy number of Eurohep (HBV standard DNA sequence containing the wild-type virus only). These diluted samples were then used for array analysis. The minimum amount (copy number/mL) of mutant strain detectable was calculated. The experiment was repeated twice for each of the five samples.

In addition to analysis of samples from Chinese patients with hepatitis B, 25 samples from patients of other ethnicities were analysed to validate the eight oligonucleotides for the determination of HBV genotypes. These samples were also assayed by the commercial kit (Inno-Lipa HBV Genotyping assay) and sequencing was performed to confirm the genotypes.

Results

Of the initial 100 HBV patients' samples analysed, 56 samples gave concordant results with mutations detected by the array as well as the Inno-Lipa HBV Genotyping assay. In 43 samples, additional mutations were detected on the array. The presence of these mutations was confirmed by sequencing.

Results of samples from most patients were concordant using both the array and the Inno-Lipa kit. In a few patients, the emergence of drug-resistant mutations was detected 3-7 months prior to overt biochemical relapse of hepatitis. This indicates the enhanced sensitivity of the array. In addition, it was possible to assay by array samples containing <60 c/mL of HBV (as the lower limit determined by the commercial quantitative PCR kit). The Table shows the results of four selected patients on longitudinal follow-up.

Serial dilutions of one serum sample with an equal amount (viral copy number) of Eurohep, PCR amplification, and analysis by the array showed that it was possible to detect the mutants down to a minimum of 139 c/mL at a dilution of 1:20 480. By diluting the first PCR product an extra 10-fold from a 1:10 240 dilution (ie final dilution of 1:102 400), it was possible to achieve a detection limit of 28 c/mL. Similar results were obtained for the other four serum samples tested.

Oligonucleotides for the detection of HBV genotypes were validated from 25 serum samples sent from our overseas collaborator. It was possible to validate oligonucleotides for genotypes A, B, C, D,

Serum sample (date taken)				
Follow-up				
III	IV	V	VI	VII
AA70 (14/6/04)	AA71 (30/6/04)	AA72 (20/10/04)	AA73 (6/4/05)	AA74 (28/7/05)
6 x10^4 c/mL (80I, 80V, 180M, 204I)	4.17 x10^4 c/mL (Adefovir↓ at 26/9/04) (80I, 80V, 180M, 204I)	1.37 x10^4 c/mL (80V, 80I, 180M, 204I)	45 x10^6 c/mL (80V, 80I, 180M, 204I)	113 x10^6 c/mL (80V, 80I, 180M, 204I) [5/06 stopped adefovir]
C: L80, 80I, 80V, V84, 84M, L180, 180M, 204I	C: L80, 80I, 80V, 180M, 204I	C: 80I, L180, 180M, 240I	C: 80I, L180, 180M, 204I	C: L80, 80I, 80V, L180, 180M, 204I
AA85 (19/10/04)	AA87 (23/11/04)	AA88 (21/12/04)		
3.45 x10^5 c/mL (80I, 80V, 180M, 204I)	7.24 x10^3 c/mL (80I, 80V, 180M, 204I)	345 c/mL (adefovir↓)		
C: 80I, 80V, L82, 82M, L180, 180M, 204I	C: 80I, 80V, L180, 180M, ?180V, 204I	C: L80, 80I (wk), T126, 126A (S gene)		
M4 (14/12/04)	M3 (30/3/06)	M5 (24/7/06)		
No polymerase chain reaction product	1.0 x10^4 c/mL (80I, 180M)	0.91 x10^2 c/mL		
B: L80, 80I, T128, 128A, L180, 180M, M204, 204I	B: 80I, T128, 128A, 180M, 204I			
N4 (14/3/06)	N5 (12/6/06)	N3 (29/9/06)		
3.79 x10^3 c/mL (80I weak)	1.85 x10^3 c/mL	549 c/mL		
C: 80I, 128A, 204I	C: 80I, 128A, 204I, T131, 131I (S gene)	C: L80, 80I, 128A, 204I, T131, 131I (S gene)		

E, and G with these samples. We failed to find any samples with genotype F and H, possibly because those are extremely rare and not associated with any of the ethnic groups we have studied.

Discussion

The HBV array in the present study has been validated through analysis of a total of 506 serum samples. It was possible to check the specificity of the majority of oligonucleotides for detecting HBV drug resistant mutations as well as genotype. The S gene mutations were rare and not encountered in many samples.

This array demonstrated improved sensitivity compared with existing commercial kits, with a detection limit down to ~28 c/mL of HBV. It enabled early detection of the emergence of drug-resistant mutants and thus timely switching to an alternative drug.

Acknowledgements

This study was supported by the Research Fund for the Control of Infectious Diseases, Food and Health Bureau, Hong Kong SAR Government (#06060572). The investigators acknowledge collaborative support from Dr G Alexander of the Addenbrooke's Hospital, University of Cambridge, United Kingdom. Prof Vivian Chan is supported by the Chui Fook Chuen Foundation.

Results from this study have been published in: Chan K, Yam I, Yuen J, et al. A comprehensive HBV array for the detection of HBV mutants and genotype. Clin Biochem 2011;44:1253-60.

A patent related to work derived from this study has been granted: Kaimin Chan, Napyee Vivian Chan, Chinglung Lai, Manfung Yuen. Hepatitis B variants with reduced sensitivity to therapeutic compounds, their detection and uses thereof. WO 2009121243 A2.

References

1. World Health Organization. Hepatitis B. World Health Organization Fact Sheet 2004. Available at http://www.who.int/mediacentre/factsheets/fs204/en/
2. Lai CL, Yuen MF. Chronic hepatitis B—new goals, new treatment. N Engl J Med 2008;359:2488-91.
3. Yuen MF, Sablon E, Hui CK, Yuan HJ, Decraemer H, Lai CL. Factors associated with hepatitis B virus DNA breakthrough in patients receiving prolonged lamivudine therapy. Hepatology 2001;34:785-91.
4. Cooreman MP, Leroux-Roels G, Paulij WP. Vaccine- and hepatitis B immune globulin-induced escape mutations of hepatitis B virus surface antigen. J Biomed Sci 2001;8:237-47.
5. Chan K, Wong MS, Chan TK, Chan V. A thalassaemia array for Southeast Asia. Br J Haematol 2004;124:232-9.

Functional significance of hepatitis B virus subgenotype Cs genomic markers

MS Li, TCK Lau, HLY Chan, SKW Tsui *

KEY MESSAGES

1. The G1613A mutation suppresses hepatitis B e antigen (HBeAg) secretion and increases the viral load.
2. The T2170G mutation decreases the extracellular concentration of HBeAg, although it has a milder effect when compared with G1613A.
3. Co-mutations of G1899A and T2170G/T2441C counteract the effect of G1613A and inhibit hepatitis B virus (HBV) DNA synthesis.
4. RFX1 plays a significant role in transactivating HBV core promoter activity with the G1613A mutation.
5. Mutations at the nt. 1613, 1899, 2170, and 2441 of the HBV genome could affect subcellular localisation of the HBV core protein.

Hong Kong Med J 2014;20(Suppl 6):S28-30
RFCID project number: 09080302

[1] MS Li, [2] TCK Lau, [3] HLY Chan, [1,4,5] SKW Tsui

[1] *School of Biomedical Sciences, The Chinese University of Hong Kong*
[2] *Department of Biology and Chemistry, The City University of Hong Kong*
[3] *Department of Medicine and Therapeutics, The Chinese University of Hong Kong*
[4] *Hong Kong Bioinformatics Centre, The Chinese University of Hong Kong*
[5] *Centre for Microbial Genomics and Proteomics, The Chinese University of Hong Kong*

* Principal applicant and corresponding author: kwtsui@cuhk.edu.hk

Introduction

Chronic hepatitis B virus (HBV) infection increases the risk of developing primary hepatocellular carcinoma (HCC); about one million people die from HBV-related diseases annually. Development of new strategies for the diagnosis and treatment of chronic HBV infection is important. In a case-control study to identify markers in the HBV genome that can be associated with HCC development, the complete HBV genomes from 200 HCC patients and controls were sequenced and genotyped; several hot-spot mutations in the HBV genome were identified as markers in each genotype.[1] In this study, four genomic markers of HBV subgenotype Cs were selected to evaluate the impact of these markers on viral DNA replication and protein synthesis.

Methods

This study was conducted from January 2010 to December 2011. Four genomic markers on HBV subgenotype Cs were selected (Table). Replication-competent HBV subgenotype Cs' clones of the wild-type HBV genome were originally extracted from the serum of an HBV-positive individual. A 1.3 x HBV genome of the Cs subgenotype was successfully constructed in the pUC18 vector. Other replication-competent HBV clones with either single or combinational mutations were subsequently constructed by site-directed mutagenesis.

The clones were then transfected into Huh7 hepatoma cells to enable viral replication. HBV surface antigen and HBV e antigen (HBeAg) were detected both in culture media and in lysate by enzyme-linked immunosorbent assay. The HBV DNA was then detected by quantitative real-time polymerase chain reaction and Southern blot analysis. To explore the impact of the mutations on HBV core antigen (HBcAg), the subcellular localisation of the HBcAg in HBV mutants was observed by using confocal microscopy.

The wild-type and G1613A mutated core promoters were cloned. The effect of the G1613A mutation on core promoter activity was evaluated by dual-luciferase reporter assay. The effect of the mutation on the binding of endogenous cellular proteins was assessed by the electromobility shift assay (EMSA).

Continuous variables were compared using *t* test or Mann-Whitney *U* test as appropriate. Categorical variables were compared using Chi-squared test or Fisher's exact test as appropriate. All statistical tests were two sided, and a P value of <0.05 were considered statistically significant.

Results

Using confocal microscopy, the localisation pattern of HBV core protein and virions in HBV-transfected Huh-7 cells was observed. Four distinct patterns of localisation were identified. Each pattern represented a stage of the life cycle during HBV replication. Although all patterns could be observed in liver cells transfected with wild-type HBV and HBV mutants, the distribution of phenotypes in some mutants was

TABLE. Summary of genomic markers in hepatitis B virus subgenotype Cs and their consequences*

Nucleotide			Promoter affected	Amino acid sequence affected	
Position	Wild-type	Mutants		Polymerase	Precore/core
1613	G	A	Negative regulatory element of core promoter	RNase H, R151K	
1899	G	A			Precore, G29D
2170	T	C/G			Core, N90N/K
2441	T	C			Core, S181P

* T2170C is a synonymous mutation that is excluded

quite different from the others.

The G1613A mutation significantly increased the level of extracellular HBV DNA by two-fold. Southern blots were performed to confirm the enhanced viral DNA production in the mutants. The level of intracellular HBV DNA intermediates was not affected, whereas the level of extracellular HBV DNA significantly increased in G1613A mutants. The G1613A mutation significantly enhanced HBV DNA synthesis. Similar tests were performed using other HBV clones. Nearly every HBV clone with G1631A mutation consistently obtained about a two-fold increase in HBV DNA level in the extracellular medium, except for the clones 1613/1899 and 1613/1899/2170/2441. Co-mutations of G1899A and T2170G/T2441C counteracted the effect of the G1613A mutation and inhibited HBV DNA synthesis.

The G1613A mutation significantly decreased the extracellular HBeAg level by up to 85% compared with the wild-type HBV. The T2170G mutation also decreased extracellular HBeAg by 50% compared with the wild-type HBV.

The G1613A mutation caused a significant increase in the core promoter activity by 57% ($P<0.003$) in Huh-7 cells. The effect was reversed in the A-to-G back mutation by 47% ($P<0.003$). Similar result was obtained in HepG2 cells, in which the core promoter activity was significantly increased by 30% ($P<0.02$). The effect was reversed in the A-to-G back mutation by 30% ($P<0.02$). Moreover, the double A1762T and G1764A basal core promoter mutation decreased the core promoter activity by 22% ($P<0.05$), which indicated that the effect of the G1613A mutation was comparable to that of the positive control, despite their effects being opposite.

To gain insight into the molecular effect of the G1613A mutation, negative regulatory element (NRE) DNA binding with nuclear proteins was studied using EMSA. Two specific DNA-protein complexes (C1 and C2) were observed when the NRE oligos were incubated with nuclear, but not cytosolic extracts, suggesting that the promoter interacted with the nuclear proteins in the cells. Moreover, the DNA binding to the nuclear proteins was in a dose-dependent manner. This implied that two different binding mechanisms were involved in NRE in the context of the G1613A mutation, and the mutation can modify the binding of two nuclear protein complexes to the NRE region.

RFX1 is one of the transcription activators that binds NREγ on the core promoter.[2,3] Moreover, the consensus binding sequences of RFX1 share extremely high homology with the sequence of NREγ subregion, from nt. 1605 to 1617.[2] The G1613A mutation on the NREγ site further matches the consensus RFX1 binding sequence, which is consistent with our result that the C2 complex showed higher affinity to mutant than wild-type DNA. RFX1 also shifts the wild-type and mutant NRE probe to the position corresponding to that in the C2 complex, suggesting that the C2 complex is possibly the RFX1-DNA complex. This only occurred in the NRE probes and not in the NS oligos and control, indicating the specificity between RFX1 and the DNA. Moreover, the G1613A mutation can alter the binding of RFX1 binding to NRE, in which the RFX1 protein favours the A1613 mutant over the wild type. This implied that the RFX1 could be one of the protein complexes for which binding to the NRE can be modulated by the G1613A mutation.

Discussion

The mutation of G1899A in the HBV genome causes G29D mutation on the precore protein, which is the precursor form of HBeAg. In this study, no significant change was observed in the HBeAg level or viral DNA synthesis in mutants with this mutation. Nevertheless, this mutation correlates with increased risk for HCC.[4]

The T2170G mutation is able to change codon 90 of the core protein from N to K. Codon 90 is exposed on the capsid surface and is near to the spike of the core protein dimer in the three-dimensional structure.[5] The mutation also falls on the cytotoxic T lymphocyte epitopes within the dimerisation domain of the protein.

The T2441C mutation causes S181P mutation at the C-terminal of the core protein, where the nucleic acid binding domain is positioned. Moreover, phosphorylation of the C-terminal serine residue is

essential for pregenomic RNA encapsidation and viral DNA replication.[6] However, the exact role of phosphorylation of this serine remains elusive.

In this study, the N90K and S181P mutations on the core protein affected the pattern of core protein localisation in hepatocytes. It was hypothesised that T2170G (N90K) mutation may disrupt the structure of the core protein and hence modify the structure of the capsid. This may affect core capsid formation and therefore the subsequent viral replication process. Moreover, the T2441C (S181P) mutation may alter the interaction between the HBV pregenomic RNA and the core protein during RNA encapsidation, and therefore affect the process of DNA replication.

In this study, the G1613A mutation led to suppression of HBeAg secretion. Emergence of the HBeAg-negative/-reduced mutant during chronic infection led to more active disease on liver histology, especially when the mutant became predominant with a high viral load in serum. The G1613A mutation, which triggered suppression of HBeAg secretion and enhancement of viral DNA production, may contribute to a more aggressive stage of liver disease.

Two main protein complexes were found to be associated with the NRE sequence of the core promoter and showed differential binding affinity towards the wild-type and mutant NRE sequences. This suggested a possible role of the G1613A mutation on regulating core promoter activity, and hence modulating viral replication and protein secretion. RFX1 was identified as binding to the G1613A mutant with higher affinity than the wild-type sequence and possessed the transactivating effect to enhance core promoter activity in liver cells. The G1613A-mutated NRE sequence shared higher homology with the consensus RFX1 binding sequence than the wild-type sequence, indicating that the higher affinity of the mutant NRE to the protein led to transactivation of the core promoter activity.

Acknowledgement

This study was supported by the Research Fund for the Control of Infectious Diseases, Food and Health Bureau, Hong Kong SAR Government (#09080302). Results from this study have been published in: Li MS, Lau TC, Chan SK, et al. The G1613A mutation in the HBV genome affects HBeAg expression and viral replication through altered core promoter activity. PLoS One 2011;6:e21856.

References

1. Sung JJ, Tsui SK, Tse CH, et al. Genotype-specific genomic markers associated with primary hepatomas, based on complete genomic sequencing of hepatitis B virus. J Virol 2008;82:3604-11.
2. Buckwold VE, Chen M, Ou JH. Interaction of transcription factors RFX1 and MIBP1 with the gamma motif of the negative regulatory element of the hepatitis B virus core promoter. Virology 1997;227:515-8.
3. Reinhold W, Emens L, Itkes A, Blake M, Ichinose I, Zajac-Kaye M. The myc intron-binding polypeptide associates with RFX1 in vivo and binds to the major histocompatibility complex class II promoter region, to the hepatitis B virus enhancer, and to regulatory regions of several distinct viral genes. Mol Cell Biol 1995;15:3041-8.
4. Liao Y, Hu X, Chen J, et al. Precore mutation of hepatitis B virus may contribute to hepatocellular carcinoma risk: evidence from an updated meta-analysis. PLoS One 2012;7:e38394.
5. Pairan A, Bruss V. Functional surfaces of the hepatitis B virus capsid. J Virol 2009;83:11616-23.
6. Melegari M, Wolf SK, Schneider RJ. Hepatitis B virus DNA replication is coordinated by core protein serine phosphorylation and HBx expression. J Virol 2005;79:9810-20.

Non-invasive algorithm for detecting advanced liver fibrosis in chronic hepatitis B patients

HLY Chan *, VWS Wong, GLH Wong, PCL Choi

KEY MESSAGES

1. Liver stiffness measurement (LSM) using FibroScan is superior to serum test formula to diagnose advanced liver fibrosis.
2. Combination of LSM and the Forns index (LSM-Forns algorithm) can improve the accuracy of LSM to predict advanced liver fibrosis.

Hong Kong Med J 2014;20(Suppl 6):S31
RFCID project number: 09080292

[1] **HLY Chan**, [1] **VWS Wong**, [1] **GLH Wong**, [2] **PCL Choi**

The Chinese University of Hong Kong:
[1] *Department of Medicine and Therapeutics*
[2] *Department of Anatomical and Cellular Pathology*

* Principal applicant and corresponding author: hlychan@cuhk.edu.hk

Chronic hepatitis B is the most important cause of liver cirrhosis in Asia. Liver fibrosis is the intermediate stage to liver cirrhosis. Determining severity of liver fibrosis is important to determine the prognosis, risk of hepatocellular carcinoma, and need for antiviral therapy. Liver biopsy is the gold standard, but it is limited by its invasiveness and risk of bleeding. Transient elastography by the Fibroscan is a non-invasive measure for severity of liver fibrosis. Liver stiffness is measured based on shear wave velocity across the liver. It is accurate to determine advanced fibrosis in chronic hepatitis B and C patients, but the accuracy for mild-to-moderate fibrosis is less optimal.[1] Various serum indices are developed to measure liver fibrosis in viral hepatitis, including aspartate aminotransferase–to-platelet ratio-index, Forns index, FIB-4, Hui index, and Fibroindex. We investigated a combined algorithm of a serum test formula with Fibroscan for the evaluation of severity of liver fibrosis in chronic hepatitis B patients. A biopsy cohort of 156 hepatitis B patients was used as the training cohort,[2] and the resultant algorithm was validated in an independent cohort of 82 patients with liver biopsy.

Liver stiffness measurement by Fibroscan was superior to that by all other serum test formulae, consistent in both the training and the validation cohorts.[3] The area under the receiver operating characteristics curve (AUROC) for Fibroscan was 0.88 (95% confidence interval [CI], 0.85-0.91, P<0.001) in the training cohort and 0.80 (95% CI, 0.68-0.92, P<0.001) in the validation cohort. Among various serum tests formulae, Forns index was best in diagnosing advanced fibrosis, with an AUROC of 0.70 (95% CI, 0.62-0.78, P<0.001) in the training cohort and 0.72 (95% CI, 0.60-0.85, P<0.001) in the validation cohort.

By combining the liver stiffness measurement and Forns index, an algorithm superior to either test was derived. A low liver stiffness or a Forns index of <5.2 could exclude >60% patients with mild fibrosis and avoided the need of liver biopsy. A high liver stiffness together with a Forns index of >8.4 could confirm advanced liver fibrosis with <1% error. This non-invasive algorithm can be conveniently used in the primary care setting, as Forns index only requires common blood tests measuring levels of platelet, gamma-glutamyl transpeptidase, and cholesterol. For patients excluded for advanced liver fibrosis, only observation is needed. For patients with uncertain liver fibrosis, they should be referred to specialist for consideration of liver biopsy. Those confirmed to have advanced liver fibrosis by the combined algorithm can proceed directly to antiviral therapy without the need of an invasive liver biopsy. With this algorithm, liver biopsy can be avoided in approximately 50% of patients.

Acknowledgements

This study was supported by the Research Fund for the Control of Infectious Diseases, Food and Health Bureau, Hong Kong SAR Government (#09080292). Results of this study have been published in: Wong GL, Wong VW, Choi PC, Chan AW, Chan HL. Development of a non-invasive algorithm with transient elastography (Fibroscan) and serum test formula for advanced liver fibrosis in chronic hepatitis B. Aliment Pharmacol Ther 2010;31:1095-103.

References

1. Wong VW, Chan HL. Transient elastography. J Gastroenterol Hepatol 2010;25:1726-31.
2. Chan HL, Wong GL, Choi PC, et al. Alanine aminotransferase-based algorithms of liver stiffness measurement by transient elastography (Fibroscan) for liver fibrosis in chronic hepatitis B. J Viral Hepat 2008;16:36-44.
3. Wong GL, Wong VW, Choi PC, Chan AW, Chan HL. Development of a non-invasive algorithm with transient elastography (Fibroscan) and serum test formula for advanced liver fibrosis in chronic hepatitis B. Aliment Pharmacol Ther 2010;31:1095-103.

Use of serum hepatitis B viral DNA in prognostication of patients undergoing non-surgical therapy for liver cancer

SL Chan *, FKF Mo, PKS Chan, W Yeo

KEY MESSAGES

1. Hepatitis B virus (HBV) load is not a prognostic factor for patients with advanced HBV-related hepatocellular carcinoma (HCC) undergoing non-surgical therapy.
2. Antiviral therapy for HBV-related HCC is associated with improved survival outcome.

Hong Kong Med J 2014;20(Suppl 6):S32-4
RFCID project number: 09080422

[1] SL Chan *, [1] FKF Mo, [2] PKS Chan, [1] W Yeo

[1] *Department of Clinical Oncology, The Chinese University of Hong Kong*
[2] *Department of Microbiology, The Chinese University of Hong Kong*

* Principal applicant and corresponding author: L_chan@clo.cuhk.edu.hk

Introduction

Chronic hepatitis B virus (HBV) infection is the most common cause of hepatocellular carcinoma (HCC) in Hong Kong. The HBV mediates hepatocarcinogenesis via its direct oncogenic effects and/or indirect mechanism of cirrhotic damage to the liver. Viral load is monitored by serum HBV DNA during treatment of chronic HBV infection; the HBV DNA level in serum is associated with risk of HCC development.[1] The clinical impact of viral load on the outcome of patients with malignancy remains unclear.

In this study, we aimed to validate the prognostic impact of baseline serum HBV DNA in patients with inoperable HCC undergoing non-surgical therapy. In addition, the impact of antiviral therapy on HBV viral load during treatment of HCC was evaluated.

Methods

This study was conducted from October 2009 to September 2010. Serum HBV DNA levels from prospectively collected serum samples of patients with inoperable HCC were analysed. Consecutive patients with inoperable HBV-related HCC who attended the Joint Hepatoma Clinic, Prince of Wales Hospital, Hong Kong, from 2004 to 2006 were included. The HBV status was confirmed by positive hepatitis B surface antigen for ≥6 months. The diagnosis was either confirmed histologically or by the presence of characteristic imaging findings in contrast scan together with α-fetoprotein of >500 ng/mL. Patients were treated according to the standard practice of the department. Patients were followed up regularly every 4 to 8 weeks, or more frequently if indicated clinically.

The blood sample on the day of diagnosis of HCC was used for quantitation of serum HBV DNA. If not available, another sample taken within 2 months and nearest to the date of HCC diagnosis was used. The HBV DNA was quantified by TaqMan real-time polymerase chain reaction assay as described previously.[2] The range of HBV DNA detection was from 102 to 109 copies/mL, with correlation coefficient of the standard curve routinely >0.990.

Antiviral therapy was defined as the use of any approved nucleoside/nucleotide analogues for HBV infection for >6 months.

Clinical factors, laboratory results and tumour factors at baseline were determined. These parameters correlated with survival using Cox's proportional hazard model to detect independent prognostic factors for overall survival. Multivariate analysis was carried out using a stepwise model building procedure based on a significance value of 0.05 for both inclusion and exclusion of prognostic factors.

Results

A total of 135 men and 15 women aged 18 to 86 (median, 60) years were analysed (Table 1). The median follow-up time was 15.0 (11.8-18.2) months. Most (71.3%) patients had multifocal intrahepatic tumours. In terms of tumour staging, 68.7% had tumour, node, metastasis (TNM) stage IV disease, 47.3% had Okuda stage B disease, and 46.8% had Chinese University Prognostic Index intermediate stage disease. About 52.7% of patients received palliative treatment (including transarterial or systemic therapy) and 42.0% received supportive care.

The median overall survival was 7.8 (95% confidence interval [CI], 5.3-9.4) months. The median serum HBV DNA level at the time of diagnosis of HCC was 6.12 (range, 2.0-9.2) $\log_{10}$ copies/mL. In

univariate analysis, serum HBV DNA at diagnosis of HCC was not prognostic of overall survival (hazard ratio [HR]=1.0; 95% CI, 0.9-1.0; P=0.13).

A total of 35 (23.3%) patients received antiviral therapy (nucleoside/nucleotide analogues) for >6 months and had better overall survival than patients who did not receive antiviral therapy (20.9 vs. 4.4 months; HR=0.22; 95% CI, 0.12-0.40; P<0.0001). Antiviral therapy remained an independent prognostic factor (HR=0.17; 95% CI, 0.09-0.32; P<0.0001) after adjusting for all factors. Patients with antiviral therapy had better liver reserves at the time of diagnosis of HCC (lower alkaline phosphatase, international normalised ratio, and bilirubin levels) and higher rates of receiving antineoplastic treatment for HCC (Table 1). The two groups did not differ significantly in terms of the HBV DNA level at the time of HCC diagnosis, TNM staging, or largest tumour diameter.

Apart from antiviral therapy, other independent prognostic factors included advanced Okuda stage, high α-fetoprotein value, presence of portal vein thrombosis, and low albumin level based on multivariate analyses (Table 2).

Discussion

In this study, the HBV viral load at baseline was not a prognostic factor for overall survival. This finding is contrary to our previous findings from another patient cohort with advanced HCC undergoing cytotoxic chemotherapy.[3] We postulated that the differences are due to different patient populations and changing practices for prescription of antiviral therapy over time. Our previous report focused on a phase III clinical trial comparing two different regimens of systemic chemotherapy.[3] Prophylactic use of antiviral therapy had not been established at the time of the previous study. Patients with higher baseline serum HBV DNA had higher risk for and/or a more severe form of HBV reactivation. Accordingly, the poorer prognosis in patients with higher baseline HBV DNA was due to poor outcome among HCC patients with HBV reactivation. In the

TABLE 1. Patient characteristics

Variable	Antiviral therapy (n=35)	Others (n=115)	Total (n=150)	P value
No. of male:female	33:2	102:13	135:15	0.3344
Median (range) age (years)	57 (18-86)	61 (26-86)	60 (18-86)	0.0932
Eastern Cooperative Oncology Group (No. [%] of patients)				0.2634
0	12 (34.3)	25 (21.7)	37 (24.7)	
1	22 (62.9)	82 (71.3)	104 (69.3)	
2	0 (0.0)	6 (5.2)	6 (4.0)	
3	1 (2.9)	2 (1.7)	3 (2.0)	
Median (range) $\log_{10}$ HBV DNA (copies/mL)	5.52 (2.0-8.64)	6.14 (2-9.04)	6.12 (2.00-9.04)	0.0576
Median (range) haemoglobin (g/dL)	13.6 (9.2-17.0)	12.6 (7.6-18.0)	12.8 (7.6-18.0)	0.0518
Median (range) white blood cells ($x10^9$/L)	5.8 (3.2-9.9)	6.6 (2.8-23.4)	6.4 (2.8-23.4)	0.0088
Median (range) platelets ($x10^9$/L)	164 (53-504)	168 (12-943)	166.5 (12-943)	0.2133
Median (range) bilirubin (μmol/L)	15 (8-98)	21 (7-824)	20 (7-824)	0.0441
Median (range) alanine transaminase (IU/L)	56 (15-434)	71 (16-432)	64.5 (15-434)	0.8253
Median (range) alkaline phosphatase (IU/L)	128 (47-434)	175 (46-749)	161.5 (46-749)	0.0219
Median (range) albumin (g/L)	38 (25-48)	35 (21-48)	36 (21-48)	0.0010
Median (range) international normalised ratio	1.07 (0.88-1.16)	1.15 (0.90-2.93)	1.14 (0.88-2.93)	0.0130
Median (range) prothrombin time (sec)	11.9 (9.5-17.4)	12.8 (10.2-32.9)	12.7 (9.5-32.9)	0.0081
Median (range) α-fetoprotein (ng/mL)	278 (1-2193000)	784 (3-3637000)	586 (1-3637000)	0.7795
Ascites (No. [%] of patients)	2 (5.7)	37 (32.2)	39 (26.0)	0.0018
Cirrhosis (No. [%] of patients)	12 (34.3)	32 (27.8)	44 (29.3)	0.4624
Vascular involvement (No. [%] of patients)	8 (22.9)	44 (38.3)	52 (34.7)	0.0936
Tumour No. (No. [%] of patients)				0.4011
Single	12 (34.3)	31 (27.0)	43 (28.7)	
Multiple	23 (65.7)	84 (73.0)	107 (71.3)	
Median (range) tumour size (cm)	4.0 (0-20)	7.5 (0-23)	7 (0-23)	0.1264

TABLE 2. Multivariate analysis

Variable	Hazard ratio (95% CI)	P value
Okuda staging system	1.57 (1.11-2.20)	0.0104
Antiviral therapy	0.17 (0.09-0.32)	<0.0001
Log_e α-fetoprotein	1.14 (1.08-1.21)	<0.0001
Portal vein thrombosis	2.72 (1.74-4.23)	<0.0001
Albumin ≤35 g/L	1.71 (1.05-2.71)	0.0299

present study, a large number of patients underwent loco-ablative therapy. It was routine practice for patients undergoing systemic chemotherapy to be given prophylactic antiviral therapy. It is therefore likely that patients with higher serum HBV DNA levels at baseline could be salvaged from HBV reactivation and hence had a better prognosis than the previous cohort.

Antiviral therapy was an independent prognostic factor for patients with HCC, even after adjusting for other prognostic factors. Antiviral therapy for patients with dual pathologies (malignancy and cirrhosis) of HCC can theoretically improve liver function and prognosis. This concept has been suggested by a case-control study[4] and a small-scale observation series.[5]

There were three limitations to the present study. First, during recruitment of the cohort, antiviral therapy was not reimbursable for most patients, and there was no consensus guideline on prescribing antiviral therapy after the diagnosis of HCC. The prescription pattern could have been subject to potential bias or unknown confounding factors. Second, serial measurements of serum viral loads were lacking, and therefore it is unclear whether and by how much the antiviral therapy exerted its viral suppressive effects during the course of HCC. The potential benefits of antiviral therapy are hypothesis generating only. Further studies are required to validate the findings. Finally, the retrospective nature of the study may have led to bias in the interpretation of data.

Conclusion

Serum HBV DNA level at baseline was not a prognostic factor for patients with inoperable HCC. Prescription of antiviral therapy at the time or after diagnosis of HCC was associated with better overall survival of patients with HCC.

Acknowledgement

This study was supported by the Research Fund for the Control of Infectious Diseases, Food and Health Bureau, Hong Kong SAR Government (#09080422).

References

1. Chan HL, Tse CH, Mo F, et al. High viral load and hepatitis B virus subgenotype ce are associated with increased risk of hepatocellular carcinoma. J Clin Oncol 2008;26:177-82.
2. Chan HL, Chui AK, Lau WY, et al. Factors associated with viral breakthrough in lamivudine monoprophylaxis of hepatitis B virus recurrence after liver transplantation. J Med Virol 2002;68:182-7.
3. Yeo W, Mok TS, Zee B, et al. A randomized phase III study of doxorubicin versus cisplatin/interferon alpha-2b/doxorubicin/fluorouracil (PIAF) combination chemotherapy for unresectable hepatocellular carcinoma. J Natl Cancer Inst 2005;97:1532-8.
4. Kuzuya T, Katano Y, Kumada T, et al. Efficacy of antiviral therapy with lamivudine after initial treatment for hepatitis B virus-related hepatocellular carcinoma. J Gastroenterol Hepatol 2007;22:1929-35.
5. Koda M, Nagahara T, Matono T, et al. Nucleotide analogs for patients with HBV-related hepatocellular carcinoma increase the survival rate through improved liver function. Intern Med 2009;48:11-7.

Human papillomavirus status in southern Chinese women

SS Liu, KKY Chan, RCY Leung, AMW Yip, LSK Lau, XY Liao, LL Jiang, MHM Luk, SST Lo, DYT Fong, ANY Cheung, ZQ Lin, HYS Ngan *

KEY MESSAGES

1. The overall and type-specific human papillomavirus (HPV) prevalence differed between Hong Kong and Guangzhou healthy women. The prevalence of HPV was significantly higher in Guangzhou than Hong Kong women. Younger women had significantly higher risk of HPV infection.
2. HPV16 remained the most common type detected in both regions; the frequency increased with increasing disease severity. The prevalence of HPV58 and HPV52 was relatively high in women with normal cervix and precancerous lesions.

Hong Kong Med J 2014;20(Suppl 6):S35-8
RFCID project number: 05050052

[1] SS Liu, [2] KKY Chan, [1] RCY Leung, [1] AMW Yip, [1] LSK Lau, [2] XY Liao, [2] LL Jiang, [3] MHM Luk, [4] SST Lo, [5] DYT Fong, [2] ANY Cheung, [3] ZQ Lin, [1] HYS Ngan

[1] *Department of Obstetrics and Gynaecology, Faculty of Medicine, The University of Hong Kong, Hong Kong*
[2] *Department of Pathology, Faculty of Medicine, The University of Hong Kong, Hong Kong*
[3] *Department of Obstetrics and Gynaecology, The Second Affiliated Hospital of Sun Yat-Sen University, Guangzhou, China*
[4] *Family Planning Association of Hong Kong, Hong Kong*
[5] *School of Nursing, Faculty of Medicine, The University of Hong Kong, Hong Kong*

* Principal applicant and corresponding author: hysngan@hkucc.hku.hk

Introduction

Human papillomavirus (HPV) is a sexually transmitted pathogen that plays an important role in the pathogenesis of precancerous cervical lesions and cervical cancer.[1] The prevalence of HPV types in Hong Kong differs from that in Sichuan, China. Cross-border travel and marriage between people in Hong Kong and Guangzhou have increased greatly, as has the potential for disease transmission.

Integration of HPV correlates with poor response to treatment and poor disease-free survival in cervical cancer.[2] Integration usually causes deletion and/or disruption of the E2 gene of the HPV. In this study, we aimed to determine (1) the spectrum and prevalence of HPV in healthy women in Hong Kong and Guangzhou, and (2) whether integration of the high-risk HPV16 and HPV58 genomes in the host is associated with progressive severity of the precancerous cervical lesion and cervical cancer.

Methods

This cross-sectional study was approved by the local institutional review board and conducted from October 2006 to September 2008, in collaboration with the Department of Obstetrics and Gynaecology and Department of Pathology of The University of Hong Kong, the Family Planning Association of Hong Kong, and the Department of Obstetrics and Gynaecology of the Second Affiliated Hospital, Sun Yet-Sen University, Guangzhou, Guangdong, China.

The prevalence of HPV and type-specific infections in healthy women and women with precancerous lesions and cervical cancer were compared between Hong Kong and Guangzhou. The association between co-factors and the risk of HPV infection was analysed. The integrations of HPV16 and HPV58 viral DNA in host genomes were assessed and the clinical significance was determined.

Cytology samples of 1280 and 1273 healthy women in Hong Kong and Guangzhou were collected, respectively. The exfoliated cervical cells were collected by ThinPrep (Hologic, Bedford, MA, USA) in Hong Kong or liquid-based cervical cytology test in Guangzhou. In addition, 438 and 204 samples of cervical precancerous lesions and cervical cancers were retrospectively selected in the two regions, respectively.

A Hybribio DNA extraction kit (Hybribio, Hong Kong) and QIAamp DNA FFPE Tissue Kit (Qiagen, Hilden, Germany) were used for DNA extraction from the cytological remnants and the paraffin-embedded tissues, respectively. Genotyping of HPV was performed using the GenoArray HPV genotyping test (Hybribio), which is a polymerase chain reaction (PCR)-based assay that is capable of amplifying 21 HPV genotypes, including 13 high-risk types (16, 18, 31, 33, 35, 39, 45, 51, 52, 56, 58, 59, and 68) and nine other-risk types.

The HPV viral DNA integration was determined by quantitative real-time fluorescent PCR with five sets of E2 and one set of E6 primers for HPV16 and HPV58. The proportion of integrated value was calculated by the ratio of E2 value (episomal) to E6 value (episomal and integrated).

Results

Of the 1280 and 1273 cytology samples from Hong

TABLE 1. Comparison of the prevalence of human papillomavirus (HPV) infections in Hong Kong and Guangzhou women

HPV prevalence	Hong Kong (% positive)				Guangzhou (% positive)			
	Normal (age-adjusted)	Low-grade cervical intraepithelial neoplasia	High-grade cervical intraepithelial neoplasia	Cervical cancer	Normal (age-adjusted)	Low-grade cervical intraepithelial neoplasia	High-grade cervical intraepithelial neoplasia	Cervical cancer
Overall prevalence	5.6‡	22.4‡	30.8	40.2	10.1‡	6.0‡	28.9	39.2
Multiple infection	1.8	1.9	0.9	1.0	1.8	0	1.8	2.0
Multiple infection among HPV-positive	33.7†	8.3	2.8	2.4	15.3†	0	6.1	5.0
High-risk HPV	4.0‡	31.0†	28.2	40.2	7.6‡	5.0†	23.7	39.2
High-risk types among HPV-positive	71.9	79.2	91.7	100	75.5	83.3	81.8	100
Type-specific (% HPV-positive)								
HPV16	23.6*	16.7	27.8	56.1*	11.0*	16.7	36.4	77.5*
HPV18	14.6*	12.5	0*	22.0	4.9*	0	15.2*	17.5
HPV31	0‡	0	13.9*	4.9	16.6‡	33.3	0*	0
HPV52	19.1	20.8	13.9	7.3	23.9	33.3	9.1	0
HPV58	20.2*	29.2†	27.8	9.8	10.4*	0†	12.1	5.0
Total (5 types)	77.5	79.2	83.4	100	66.8	83.3	72.8	100

* P=0.01 to <0.05, Chi-squared test
† P=0.001 to <0.01, Chi-squared test
‡ P<0.001, Chi-squared test

Kong and Guangzhou women, respectively, 1245 (97.3%) and 1209 (95.0%) had normal cytology. The age-adjusted HPV prevalence was significantly lower in Hong Kong than Guangzhou women (5.6% [89/1245] vs 10.1% [163/1209], Table 1), particularly in the three younger age-groups (Fig). The prevalence of HPV infection varied between age-groups in the two regions.

In Hong Kong, the HPV prevalences in women with low-grade cervical intraepithelial neoplasia (LG CIN), high-grade CIN (HG CIN), and cervical cancer were 22.4%, 30.8%, and 40.2%, respectively. In Guangzhou, the corresponding prevalences were 6.0%, 28.9%, and 39.2%, respectively. The HPV prevalence in women with LG CIN was significantly higher in Hong Kong than Guangzhou (P<0.001). The rate for age-adjusted multiple HPV infection was 1.8% in women with normal cervix for both regions, accounting for 33.7% and 15.3% of HPV-positive cases in Hong Kong and Guangzhou cohorts, respectively (P=0.001).

In Hong Kong, HPV16 was most commonly identified in women with normal cytology, HG CIN, and cervical cancer, whereas HPV58 was most commonly identified in women with LG CIN. In Guangzhou, HPV16 was most commonly identified in women with HG CIN and cervical cancer, whereas HPV52 and HPV31 were most commonly identified in women with normal cytology and LG CIN. HPV16, 52 and 58 were the most common high-risk types detected in women with normal cytology in both regions. The frequency of HPV16 in women with normal cervix and cervical cancer was significantly higher in Hong Kong than in Guangzhou (P=0.015 and P=0.036, respectively). The frequency of HPV16 increased with an increase of disease severity. The frequencies of HPV58 and 52 were higher in women with normal cervix and precancerous lesion in both regions.

Age was a risk factor only in Hong Kong women younger than 29 years, compared with other age-groups (P=0.009). Previous Pap smear test was another risk factor for women in Hong Kong (P=0.037). Women with a previous abnormal Pap smear test also had significantly higher HPV infection (P=0.021). In Guangzhou, women with previous abnormal cytological findings also had increased risk

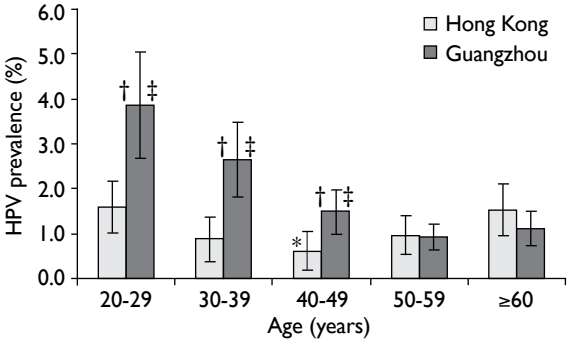

FIG. Age-adjusted human papillomavirus (HPV) infection prevalences in five age-groups in Hong Kong and Guangzhou women.

* In Hong Kong, the prevalence of HPV infection is significantly lower in the age-group of 40-49 years than that of 20-29 years and ≥60 years (P<0.05)
† The prevalence of HPV infection is significantly higher in Guangzhou than Hong Kong women in the age-groups of 20-29 years (P<0.001), 30-39 years (P<0.001), and 40-49 years (P=0.009)
‡ In Guangzhou, the prevalence of HPV infection is significantly higher in the age-groups of 20-29 years, 30-39 years, and 40-49 years than in the other groups (P<0.05)

of HPV infection (P=0.044). Two sexual behaviour variables (lifetime number of sexual partners and age at first sexual intercourse) were associated with the risk of HPV infection. In Guangzhou, the risk of HPV infection was significantly higher in women with ≥3 than 1-2 lifetime sexual partners (P<0.001). In Hong Kong, women having first sexual intercourse before the age of 20 years had higher risk than those having first sexual intercourse after the age of 21 years (P=0.043). After multivariable analysis, only the lifetime number of sexual partners remained a significant factor in Guangzhou women (Table 2). No association was noted with variables of gravidity, use of condom or oral contraceptive, history of sexually transmitted diseases, and smoking.

The complete episomal form was found in only 3/110 (2.7%) HPV16- and 4/48 (8.3%) HPV58-positive samples. HPV16 integration and HPV58 integration were detected in 107 and 44 samples, respectively; 30 (27.3%) HPV16-positive samples and only one (2.1%) HPV58-positive sample showed complete integration. No significant difference in the integration patterns of HPV16 or HPV58 with regard to the various grades of cervical lesions was noted. The distribution and frequency of HPV16 or HPV58 DNA integration were similar between the Hong Kong and Guangzhou regions.

Discussion

In Guangzhou, the age-adjusted HPV infection rate was 10.1% in women with normal cytology, which is

TABLE 2. Multiple logistic regression for risk factors of human papillomavirus (HPV) infection in Hong Kong and Guangzhou women

Variable	Hong Kong				Guangzhou			
	No.	HPV-positive (%)	OR (95% CI)	P value	No.	HPV-positive (%)	OR (95% CI)	P value
Age (years)				0.025				0.626
20-29	248	10.9	1		233	15.0	1	
30-39	243	4.9	0.53 (0.24-1.15)		237	14.3	1.48 (0.79-2.77)	
40-49	249	3.2	0.37 (0.14-1.00)		236	12.7	1.19 (0.61-2.33)	
50-59	250	7.2	0.77 (0.29-2.01)		253	13.8	1.55 (0.77-3.10)	
≥60	255	9.4	1.32 (0.50-3.48)		250	11.6	1.21 (0.59-2.49)	
Previous Pap smear test				0.038				0.087
Yes	1040	6.4	1		377	11.4	1	
No	205	10.7	0.49 (0.25-0.96)		832	14.4	0.71 (0.48-1.05)	
Lifetime number of sexual partner				0.973				0.015
1	868	6.8	1		1039	12.4	1	
2	185	7.0	0.92 (0.45-1.88)		123	13.8	1.21 (0.67-2.18)	
≥3	192	8.9	0.98 (0.46-2.09)		46	34.8	3.20 (1.45-7.04)	
Age at first sexual intercourse (years)				0.236				0.701
≤20	430	17.8	1		176	14.2	1	
21-25	510	5.3	0.55 (0.30-1.00)		643	14.3	1.31 (0.76-2.26)	
26-35	292	6.2	0.62 (0.30-1.28)		385	11.7	1.11 (0.58-2.10)	
≥36	13	7.7	1.14 (0.13-10.26)		5	20.0	1.64 (0.17-16.20)	
Sexually transmitted disease history				0.95				0.368
Never	1214	7.2	1		1170	13.2	1	
Ever	16	6.3	0.94 (0.12-7.52)		17	29.4	1.74 (0.52-5.76)	
Oral contraceptive use				0.197				0.588
Never	551	6.5	1		1031	13.2	1	
Ever	683	7.6	1.38 (0.85-2.26)		177	14.6	1.14 (0.71-1.84)	
Condom use				0.152				0.888
Never or rare	672	8.3	1		877	13.7	1	
Regular	549	5.6	0.69 (0.42-1.15)		318	12.9	0.97 (0.64-1.47)	
Gravidity				0.065				0.348
0	354	6.5	1		86	20.9	1	
1-2	455	8.4	1.87 (0.92-3.80)		548	12.4	0.55 (2.80-1.08)	
3-4	334	7.2	1.25 (0.52-3.00)		455	13.6	0.52 (0.24-1.09)	
≥5	100	4.0	0.55 (0.45-2.04)		120	12.5	0.52 (0.21-1.28)	
Smoking				0.808				0.958
Never	1105	6.7	1		1173	13.3	1	
Former	72	8.3	1.09 (0.43-2.77)		17	17.6	1.22 (0.32-4.65)	
Current	68	11.8	1.34 (0.56-3.21)		19	21.1	1.01 (0.30-3.49)	

similar to other regions of China.[3] In Hong Kong, the rate was significantly lower at 5.6%. In Guangzhou, younger women (age <39 years) had a significantly higher infection rate than older women. In Hong Kong, the highest infection rate was in women in the age-groups of 20-29 years and >60 years. The difference in HPV prevalence between the two regions could be due to differences in the living environments and life-styles.

In Hong Kong, the crude HPV infection rate in healthy women was 7.2%, which was lower than that in our previous study.[3] The difference could be due to the different HPV detection methods used. The Hybribio HPV genotyping test detects only 21 HPV genotypes, whereas the DNA sequencing method detects more genotypes. In CIN and cancer samples, the HPV prevalence was also significantly lower in our study than in the previous study. These CIN and cancer samples were paraffin-embedded tissues, and the DNA extracted was frequently fragmented. As the primers in the Hybribio HPV genotyping test amplify 450 bp long products, a number of HPV-positive samples and genotypes might have been missed.

HPV16 remained the most common high-risk type detected in both Hong Kong and Guangzhou, and HPV18 was the second most common type in cervical cancer. The frequency of HPV16 increased with increased disease severity. Consistent with our previous finding,[3] high prevalence of HPV58 and HPV52 was noted, especially in the normal and precancerous groups.

Having previous cervical cancer screening was an independent risk factor associated with HPV infection in Hong Kong women, but not in Guangzhou women. This might be due to the small sample size. Only one third of women in Guangzhou had a previous Pap smear test, compared with >80% of women in Hong Kong. This might have contributed to the higher incidence of HPV infection in healthy women in Guangzhou. Cervical cancer screening should be promoted to prevent cervical disease.

In Guangzhou, women having ≥3 lifetime sexual partners had increased risk of HPV infection. In Hong Kong, sexual behaviour factors had no such association. A population-based study in Shanxi, China also found no such association.[4]

Integration of HPV16 into the host DNA has been proposed as a potential marker of cervical neoplastic progression.[2] E2 disruption may occur in any part of the E2 genome, which spans about 1000 bp. To optimise the test sensitivity, we designed five sets of primers to flank the entire E2 sequence for HPV16 or HPV58 genes. Most of the HPV16-positive samples harboured mixed forms of viral integration products. The mixed integrated form of HPV16 was the most prevalent physical state in normal cytology, and the complete integrated form occurred in two thirds of LG CIN cases. Similar findings have also been reported.[5]

In this study, the prevalent physical state of HPV58 integration was the mixed integrated form. HPV58 commenced early during the course of lesion progression, but this might not be essential for the development of HPV58-related cervical cancer.

Significant differences in HPV16 and HPV58 integration patterns were not observed between Hong Kong and Guangzhou women, although the prevalence for both types was significantly higher in Hong Kong women. Clinical association with abnormal cytology was not observed with integration. This may have been due to the limited number of mixed swap samples and archived paraffin samples analysed. The significant portion of normal cytology samples harbouring the mixed integration form suggested that HPV16 or HPV58 integration occurred early in the cervical transformation process leading to deregulated expression of the E6/7 oncoproteins resulting in major genomic instability in HPV-infected cells. Therefore, detection of viral DNA integration may have prognostic value in the prediction of cervical lesion progression, especially in women without detectable cervical abnormality.

Acknowledgements

This study was supported by the Research Fund for the Control of Infectious Diseases, Food and Health Bureau, Hong Kong SAR Government (#05050052). We thank all doctors, research and technical staff, and participants who contributed to this project. Special thanks to Dr HJ Zhang in the Department of Pathology, The University of Hong Kong for assessment of the haematoxylin and eosin slide, Ms Elaine Szeto in the Cytology Laboratory, Department of Pathology, Queen Mary Hospital for coordination of the cytology tests, and Hybribio Ltd for technical support in HPV genotyping. We also thank the Family Planning Association of Hong Kong and Kwong Wah Hospital Well Women Clinic for participant recruitment.

References

1. Schiffman MH, Bauer HM, Hoover RN, et al. Epidemiologic evidence showing that human papillomavirus infection causes most cervical intraepithelial neoplasia. J Natl Cancer Inst 1993;85:958-64.
2. Jeon S, Allen-Hoffmann BL, Lambert PF. Integration of human papillomavirus type 16 into the human genome correlates with a selective growth advantage of cells. J Virol 1995;69:2989-97.
3. Liu SS, Tsang PC, Chan KY, et al. Distribution of six oncogenic types of human papillomavirus and type 16 integration analysis in Chinese women with cervical precancerous lesions and carcinomas. Tumour Biol 2008;29:105-13.
4. Dai M, Bao YP, Li N, et al. Human papillomavirus infection in Shanxi Province, People's Republic of China: a population-based study. Br J Cancer 2006;95:96-101.
5. Kulmala SM, Syrjanen SM, Gyllensten UB, et al. Early integration of high copy HPV16 detectable in women with normal and low grade cervical cytology and histology. J Clin Pathol 2006;59:513-7.

Cervical cancer screening by enhanced cytology: application of novel markers

ANY Cheung *, XY Guan, HYS Ngan

KEY MESSAGES

1. p634A4, TAp73, and DJ-1 immunocytochemistry as well as in situ hybridisation for the *OSMR1, PAPD7/POLS, PRAKK1*, and *TRIO* genes helped to identify cervical carcinoma and high-grade precursor cells.
2. p634A4 immunoreactivity is a potential marker for triage of atypical squamous cells of undetermined significance.
3. TAp73 immunoreactivity is a potential marker for triage of low-grade squamous intraepithelial lesions.

Hong Kong Med J 2014;20(Suppl 6):S39-43
RFCID project number: 06060642

[1] **ANY Cheung ***, [2] **XY Guan**, [3] **HYS Ngan**

The University of Hong Kong, Queen Mary Hospital:
[1] *Department of Pathology*
[2] *Department of Clinical Oncology*
[3] *Department of Obstetrics and Gynaecology*

* Principal applicant and corresponding author: anycheun@pathology.hku.hk

Introduction

Cervical cytological examination is the most widely applied screening method for cervical cancer and its precursors. Liquid-based cytology produces good-quality smears[1] and enables the use of ancillary laboratory techniques to distinguish neoplastic from benign cells.[1]

Immunohistochemical and molecular markers have been tested to identify dysplastic cells in cervical smears. When testing for human papillomavirus (HPV) or chromosome aneusomy, *MIB1* (Ki67) and p16 immunocytochemistry helps to highlight dysplastic or cancer cells.[2] Such markers may be useful for triage of patients with borderline smears of atypical squamous cells of undetermined significance (ASCUS), which is the most common abnormal cytological finding and is associated with a significantly higher risk of developing cervical cancer and its high-grade precursors.

In this study, immunocytochemical markers (*p63, p73, Eif-5A2*, and *DJ-1* genes) were tested in cervical cancer screening using immunocytochemistry and chromogenic in situ hybridisation. Differential expression of these genes in cervical cytology is useful in diagnosing cervical cancer.

p63 and *p73* genes are members of the *p53* family and play important roles in carcinogenesis. Different isoforms of p63 and p73 can enhance or suppress neoplastic cell growth. Differential expression of p63 and p73 isoforms was reported in normal and neoplastic cervical epithelium. *p73* expression is associated with radiosensitivity of cervical cancer.[3] In a study of frequently amplified regions at 3q26.2, *Eif-5A2* was found to be important in ovarian carcinogenesis.[4] Similar regions at chromosome 3q have also been identified in cervical cancer. *Eif-5A2* is a potential marker for cervical cancer. *DJ-1* has been identified as a suppressor of *PTEN*, which is a tumour suppressor gene. *DJ-1* overexpression has been noted in human malignancies compared with healthy tissue.

Novel genes can be identified in specific chromosome regions by array comparative genomic hybridisation. In our previous studies on cervical cancer samples and cell lines, the frequently amplified regions were 1q, 3p, 3q, and 5p.[5] Besides *Eif-5A2*, eight gene loci can be identified and the amplification status can be detected by chromogenic in situ hybridisation. This study aimed to assess the application value of adjunct markers in liquid-based cervical cytology for detection of carcinoma cells and precursors.

Methods

This study was conducted from March 2007 to February 2009. Residues of liquid-based ThinPrep Pap Test (Hologic, Bedford, MA, US) cervical cytology samples of high-grade squamous intraepithelial lesions (HSIL) [n=80], low-grade SIL (LSIL) [n=100], ASCUS (n=200), invasive cervical carcinoma (n=40), and healthy tissue (n=60) findings were retrieved from the Cervical Cytology Laboratory, Queen Mary Hospital, University of Hong Kong for immunocytochemistry and in situ hybridisation.[1] Cervical cancer cell lines HeLa, SiHa, ME180, and C4-1P3 as well as the ovarian cancer cell line UACC1895 were used as controls. Expression of *p63, p73, Eif-5A2*, and *DJ-1* genes was studied immunocytochemically.

To identify the eight target genes for chromogenic in situ hybridisation experiments, quantitative real-time polymerase chain reaction (PCR) using DNA extracted from healthy tissue (n=6), HSIL (n=14), and squamous cell carcinoma (SCC) [n=12] cytology samples was performed. The DNA probes for *Eif-5A2* and the eight other selected gene loci on 1q, 3p, 3q, and 5p were labelled with biotin, and chromogenic in situ hybridisation was performed. The subsequent cytology and colposcopic histology findings of the cases were traced. The HPV molecular test results, if available, were also retrieved for correlation.

Apart from *Eif-5A2*, potential genes located on 1q, 3p, 3q, and 5p for in situ hybridisation were explored through literature review followed by screening by quantitative PCR (qPCR).[5] The genomic sequences of potential target genes were retrieved from the UCSC Genome Browser (http://genome.ucsc.edu/cgi-bin/hgGateway). Primers were designed using NCBI/Primer-BLAST (http://www.ncbi.nlm.nih.gov/tools/primer-blast/). qPCR was performed on DNA extracted from pilot samples with ABI Prism 7700 Sequence Detection System (Applied Biosystems, Foster City, CA, USA).

After screening by real time PCR, eight genes with demonstrable amplification status in the cervical cancer samples were selected for chromogenic in situ hybridisation. These included *MUC1* (on 1q), *MST1R* (on 3p), *DVL3* and *FGF12* (on 3q), and *OSMR1, PAPD7/POLS, PRAKK1*, and *TRIO* (on 5p). The probes were designed and manufactured using the assay services of Empire Genomics (New York, NY, USA). Bacterial artificial chromosome clones for these eight genes and non-repetitive sequences of *MAN2A1* on chromosome 5, which acted as control for the genes on chromosome 5, were prepared. The location and clone percent coverage are listed in the Table. Plasmids containing pericentromeric regions for chromosomes 1 and 3 were used as controls for the genes on these chromosomes. After culture, the plasmid DNA was isolated by the alkaline lysis method followed by biotin labelling using BioPrime DNA Labeling System (Invitrogen; Life Technologies, Paisley, UK).

Chromogenic in situ hybridisation was performed following established protocols.[2] The slides were first incubated with 0.1% Triton X-100 and proteinase K. The labelled probes were added to the hybridisation mix, followed by overnight hybridisation. Immunocytochemistry was performed to visualise in situ hybridisation signals by peroxidase activity. Known positive and negative control slides were included in each batch of experiments. The morphology of the nuclei was taken into consideration during evaluation of in situ hybridisation signals.

Regarding immunocytochemistry, mouse anti-human *p63* (Clone 4A4; Dako, Glostrup, Denmark), mouse anti-human *TAp73* (Zymed Laboratories, San Francisco, CA, USA), DJ-1 (a gift from Prof Tak W Mak, Ontario Cancer Institute, Toronto, Canada), and mouse monoclonal antibody to *EIF-5A2* (ab57421; Abcam, Cambridge, MA, USA) were applied to the ThinPrep thin-layer cytology slides. Immunocytochemical studies were performed using the EnVision+ Dual Link System (Dako, Carpinteria, CA, USA). A light haematoxylin counterstain was used. Appropriate negative and positive controls were included. A modified Wentzensen scoring system incorporating morphologic criteria for the assessment of the immunoreactivity of the cells was used.

Chi-squared test (2-tailed) was used to compare the immunocytochemical and in situ hybridisation signals among the healthy tissue, ASCUS, LSIL, HSIL, and cervical carcinoma groups. A P value of <0.05 was considered statistically significant.

Results

Immunocytochemistry

p634A4 protein expression was found mainly at the nuclei, although weak cytoplasmic expression

TABLE. Location and clone percent coverage of in situ hybridisation probes

Gene	Chromosome	Clone	Clone percent coverage (%)	Chromosome start and stop location
DVL3	3q	RP11-814O14	100	185355977-185374008
Eif-5A2	3q	RP11-115J24	93.5	172090216-172251852
FGF12	3q	RP11-767C10	73.2	193362761-193557602
MST1R	3p	RP11-915H6	100	49782629-49932767
MUC1	1q	RP11-263K19	100	153361602-153541655
OSMR	5p	RP11-113D9	100	38808720-38981485
PAPD7	5p	RP11-681G24	100	6761120-6934896
PRKAA1	5p	RP11-357L11	100	40786785-40949438
TRIO	5p	RP11-481M12	53.7	14308043-14504474
MAN2A1	5q	RP11-259F13	95.3	109057383-109227354

was detected focally (Fig 1a). Significantly higher p634A4 expression was found in HSIL or carcinoma when compared with ASCUS and LSIL (P<0.05). Among ASCUS, p634A4 expression in cases that subsequently progressed to LSIL (P<0.05) or HSIL (P<0.05) was significantly higher than those that did not. For ASCUS positive for high-risk HPV detected by hybrid capture II, cases with a high p634A4 index were more likely to have subsequent HSIL detected (P<0.05).

TAp73 protein expression was found mainly at the nuclei, although weak cytoplasmic expression was detected focally (Fig 1b). Significantly higher TAp73 expression was found in HSIL or carcinoma when compared with ASCUS and LSIL (P<0.05). Among LSIL, significantly higher TAp73 (P<0.05) was found in cases that subsequently progressed to HSIL. TAp73 correlated with the p634A4 indices (P<0.0001).

DJ-1 protein expression was found at both the cytoplasm and the nucleus of SCC cells, whereas the healthy squamous cells were negative for DJ-1 protein. There was a significant difference in DJ-1 expression among the different diagnostic categories of healthy tissue, ASCUS, LSIL, HSIL, and SCC (P<0.05). Significantly higher DJ-1 expression was found in HSIL and SCC than in ASCUS and LSIL (P<0.05).

No significant Eif-5A2 protein expression was detected in SCC, HSIL, LSIL, and ASCUS cells. Only a few HSIL, LSIL, and ASCUS cells in a small number of samples showed weak Eif-5A2 expression. In contrast, strong expression of Eif-5A2 was demonstrated in the control ovarian cancer cell line UACC1895.

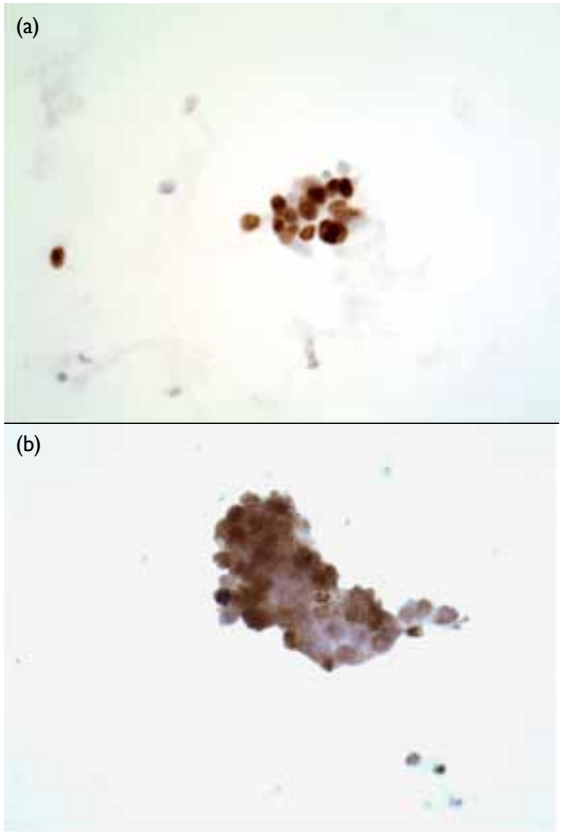

FIG 1. Overexpression of (a) p634A4 and (b) TAp73 in squamous cell carcinoma cells

Chromogenic in situ hybridisation

There were two to 14 copy signals for *DVL3* and three to 10 copy signals for *FGF12*, both on chromosome 3q, and two to 10 copy signals for *MST1R* on chromosome 3p detected in SCC and HSIL samples. Aneusomy of chromosome 3 was suggested by the multiple (2-8) copy signals for chromosome 3 centromere. There was no significant increase in the ratio of *DVL3, FGF12*, and *MST1R* to centromere 3 in SCC and HSIL samples (P>0.05), indicating no significant amplification of these genes in SCC and HSIL.

No increase in in situ hybridisation signals for *Eif-5A2* (on chromosome 3q) could be detected in carcinoma, HSIL, LSIL, and ASCUS cells. In contrast, multiple copy signals were found in the control ovarian cancer cell line UACC1895.

There were two to 10 copy signals for *MUC1* on chromosome 1q detected in SCC and HSIL samples. Aneusomy of chromosome 1 was suggested by the multiple (2-7) copy signals for chromosome 1 centromere. There was no significant increase in the *MUC1* to centromere 1 ratio in SCC and HSIL samples (P>0.05) suggesting absence of amplification of the *MUC1* gene in these lesions.

Overall, three to eight copy signals for *OSMR* and *PRAD7/POLS* each, and two to 10 copy signals for *PRKAA1* and *RIO* each on chromosome 5p were detected in SCC and HSIL samples, whereas two copy signals for the non-replicating *MAN2A-1* gene on chromosome 5 were detected (Fig 2). There was a significant increase in the ratio of *OSMR, PRAD7/POLS, PRKAA1*, and *TRIO* to centromere 5 in SCC and HSIL samples (P<0.05) suggesting amplification of these genes in SCC and HSIL.

Specificity of predicting cervical lesions

When compared with the high-risk HPV test, p634A4 immunocytochemistry increased the specificity and positive predictive value, although the sensitivity and negative predictive value were reduced.

Discussion

The selected gene loci have been found to occupy essential niches in cervical carcinogenesis. Among the six major hallmarks of cancer, these genes have been found to play a role in evading apoptosis (*p63,*

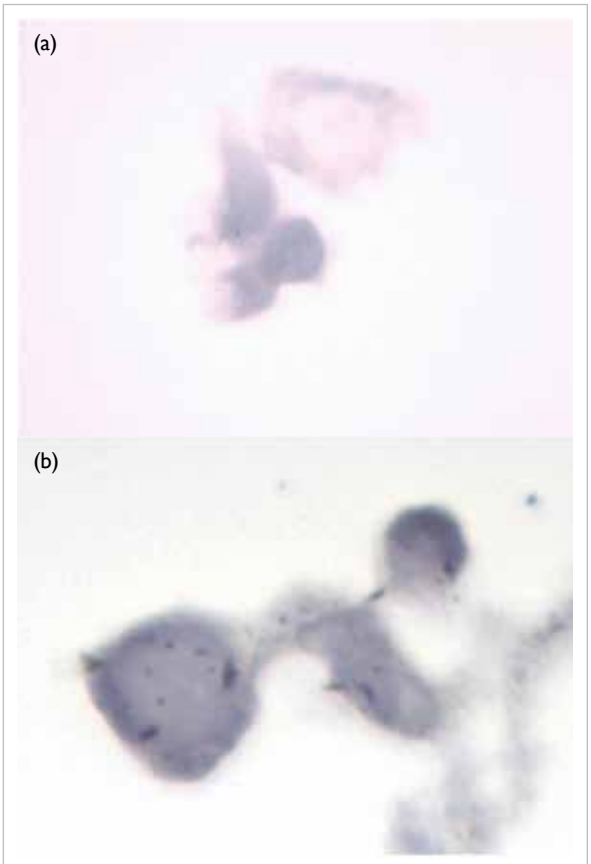

FIG 2. Amplification of *TRIO* is reflected by increases in in situ hybridisation signals for (a) *MAN2A1* and (b) *TRIO*

p73, DJ-1, TRIO, Eif-5A2), self-sufficiency in growth signals (*DVL3, FGF12, MST1R, OSMR, PAPD7/POLS*), insensitivity to anti-growth signals (*p63, p73, DJ-1, MUC1, PAPD7/POLS*), and sustained angiogenesis (*PRKAA1*).

In this study, the potential of p63 and p73 in highlighting SCC and HSIL, and in triaging ASCUS and LSIL (even among HPV-positive cases for ASCUS) was demonstrated. Nonetheless, the application of p63 and p73 immunocytochemistry, particularly p63, may have limitations for detecting glandular lesions in cervical cytology.

High expression of *DJ-1* rendered cells resistant to apoptosis and overexpression of *DJ-1* has been reported in various human cancers. In this study, high *DJ-1* expression was also found in SCC and HSIL, suggesting its role as cancer marker. However, *DJ-1* cannot be used to triage ASCUS or LSIL cases for subsequent development of HSIL or SCC.

Overexpression of *Eif-5A2* has been reported in several cancers, suggesting it is a potential oncogene. Almost all of the carcinomas with overexpression of *Eif-5A2* were adenocarcinomas. In our pilot study, *Eif-5A2* was found to be overexpressed in cervical adenocarcinoma, but to a much lesser extent in SCC. Overexpression or amplification of *Eif-5A2* was not detected in the cervical cytology samples. Tissue-specific functions of the *Eif-5A2* isoform may exist. Different gene expression profiles for adenocarcinoma and SCC have been demonstrated.

Dishevelled (*Dvl*) family gene products, cytoplasmic mediators of the Wnt/beta-catenin signalling pathway, are important in embryological development. *DVL3* was found to be overexpressed in cancers relative to metastatic ability. Nevertheless, amplification of *DVL3* was not detected in cervical cancers in this study.

In oesophageal SCC, *FGF12* was found to be associated with cellular migration, proliferation, and inhibition of apoptosis. Expression of *FGF12*, related to the MAPK signalling pathway, was validated by tissue microarray. Amplification of *FGF12* has not been reported in cervical cancers and was not detected in the cytology samples of cervical cancers in our study.

MST1R, which maps at 3p21.3, encodes a tyrosine kinase receptor closely related to the *MET* gene, whose mutations and dysregulated expression are associated with cancers of the lung and breast in association with metastasis and death. *MST1R* forms a complex with the epidermal growth factor receptor and acts as a transcriptional regulator in response to stress signals imposed on cancer cells. Nevertheless, amplification of *MST1R* was not detected in cervical cancers in this study.

Frequent amplification of *MUC1* at 1q has been reported in cancers of the breast, ovary, and thyroid in association with aggressive clinical behaviour and resistance to chemotherapy. High *MUC1* expression has been reported in cervical cancers, predominantly in adenocarcinoma. In this study, amplification of *MUC1* was not demonstrated in cytology samples of SCC and HSIL.

Amplification of *OSMR* at 5p has been reported in SCC of the cervix, adversely influencing overall patient survival independently of tumour stage. *OSMR* could activate downstream signalling pathways, including STAT3 and MAPK, and induce transcription of the angiogenic factor vascular endothelial growth factor. Our study confirmed the amplification of *OSMR* in SCC and HSIL cytology samples.

The *PAPD7/Pols* gene, which encodes a DNA polymerase, is necessary for chromosome segregation and establishing sister chromatid cohesion after S-phase. These processes are important for regulation of the cell cycle. Amplification of *PAPD7/Pols* has been demonstrated in cervical cancers as well as soft-tissue sarcomas. Amplification of *PAPD7/Pols* was also detected in SCC and HSIL cytology samples in this study.

The *PRKAA1* gene codes for the catalytic alpha 1 subunit of the AMP-activated protein kinase,

which is an important cellular metabolic stress regulator. Amplification and overexpression of *PRKAA1* has been reported in our earlier studies of cervical cancers, supporting its potential in cervical carcinogenesis. The amplification was confirmed by chromogenic in situ hybridisation in this study.

Amplification of *TRIO* at 5p15.2 has been demonstrated in oral, oesophageal, and urinary bladder cancers, in association with aggressive tumour growth and proliferation and reduced apoptosis. *TRIO* amplification is also found in primary cervical cancers, adversely influencing patients' survival. Amplification of *TRIO* was confirmed in this study.

Study limitations

This study was limited to evaluation of gene expression and amplification in SCC and squamous lesions in cervical cytology. Adenocarcinoma and its precursors were not studied.

Conclusion

In liquid-based cytology samples, TAp73, p634A4, and DJ-1 immunocytochemistry and detection of amplified gene copies of *OSMR1, PAPD7/POLS, PRAKK1*, and *TRIO* by in situ hybridisation together with morphological assessment could distinguish cervical cancer from its high-grade precursors. In addition, p634A4 and TAp73 immunoreactivity correlated with subsequent detection of HSIL or SCC in patients with ASCUS and LSIL, respectively, with enhanced specificity. p634A4 and TAp73 immunoreactivity may thus be potential markers for triage of borderline and low-grade cervical smears. Such adjunct markers can identify at-risk patients and reduce unnecessary referral for colposcopy.

Acknowledgements

This study was supported by the Research Fund for the Control of Infectious Diseases, Food and Health Bureau, Hong Kong SAR Government (#06060642). The high-risk HPV Hybrid Capture 2 test was supported by the SK Yee Medical Foundation. The authors thank Dr Kar-Fai Tam for his help in collecting clinical samples and Dr Stephanie Liu for the cervical cancer cell lines HeLa, C4-1, SiHa, ME180, and C33A. We also thank Miss Lily Fung and Miss Candy Lau for their secretarial and clerical support, and all colleagues, doctors, technical staff, patients, and participants who contributed to this project.

References

1. Cheung AN, Szeto EF, Leung BS, Khoo US, Ng AW. Liquid-based cytology and conventional cervical smears: a comparison study in an Asian screening population. Cancer 2003;99:331-5.
2. Cheung AN, Chiu PM, Tsun KL, Khoo US, Leung BS, Ngan HY. Chromosome in situ hybridisation, Ki-67, and telomerase immunocytochemistry in liquid based cervical cytology. J Clin Pathol 2004;57:721-7.
3. Liu SS, Leung RC, Chan KY, et al. p73 expression is associated with the cellular radiosensitivity in cervical cancer after radiotherapy. Clin Cancer Res 2004;10:3309-16.
4. Guan XY, Fung JM, Ma NF, et al. Oncogenic role of eIF-5A2 in the development of ovarian cancer. Cancer Res 2004;64:4197-200.
5. Huang FY, Chiu PM, Tam KF, et al. Semi-quantitative fluorescent PCR analysis identifies PRKAA1 on chromosome 5 as a potential candidate cancer gene of cervical cancer. Gynecol Oncol 2006;103:219-25.

Integrated human papillomavirus analysis as an adjunct for triage of atypical cervical cytology

ANY Cheung *, OG Wong, KKY Chan, MS Yang, CH Tsang, SL Ji, CK Lo, E Szeto, E Wong, HYS Ngan

KEY MESSAGES

1. Human papillomavirus (HPV) genotyping, HPV type-specific E6/E7 transcript detection, and hTERT transcript detection could improve the specificity of predicting subsequent development of squamous intraepithelial lesions, compared with cocktail HPV DNA detection alone.
2. The correlation between HPV RNA and hTERT expression supports their interactive role in the development of cervical cancer and precursor lesions.
3. Prophylactic HPV vaccines, besides protecting against cervical cancer, can also reduce the burden of screening for those with atypical squamous cells of undetermined significance.

Hong Kong Med J 2014;20(Suppl 6):S44-7
RFCID project number: 07060562

[1] **ANY Cheung *, [1] OG Wong, [1] KKY Chan, [2] MS Yang, [2] CH Tsang, [2] SL Ji, [1] CK Lo, [1] E Szeto, [1] E Wong, [3] HYS Ngan**

[1] *Department of Pathology, The University of Hong Kong, Queen Mary Hospital*
[2] *Department of Biology and Chemistry, City University of Hong Kong*
[3] *Department of Obstetrics and Gynaecology, The University of Hong Kong, Queen Mary Hospital*

* Principal applicant and corresponding author: anycheun@pathology.hku.hk

Introduction

Cervical cytology screening is effective for prevention of cervical cancer by detecting cervical cancer and its precursors—squamous intraepithelial lesions. The most common abnormal cytological finding encountered is atypical squamous cells of undetermined significance (ASCUS), which is associated with the risk of harbouring cervical cancer and its precursors.[1] The large number of ASCUS cases is a considerable burden for any screening programme.

High-risk human papillomaviruses (HPV) are carcinogens of cervical cancer. For triage of women with ASCUS, the Hybrid Capture 2 test (HC2) is most widely applied. When the ASCUS samples are positive for HPV, the women can be referred for colposcopy directly. When the samples are negative, women can return to cytology screening. This practice enables early referral for colposcopy and earlier diagnosis of serious cervical lesions. To improve the specificity of the HPV cocktail test, HPV genotyping, HPV transcription status, and evaluation of telomerase activity are potential adjunctive indicators.

HPV genotyping can be performed by polymerase chain reaction (PCR) using type-specific or consensus primers and sequencing, HPV DNA chips, or linear blots.[2] In addition, SNIPER HPV Genotyping Biochip Assay (previously named microarray-in-microwell assay) has been developed locally.[3] Active HPV infection can be detected by assessing RNA transcription of two HPV oncogenes—E6 and E7—that interact with two important tumour suppressor genes—p53 and RB—respectively. Among women with ASCUS, HPV RNA transcription may potentially identify high-grade cervical lesions.[4] Telomerase adds telomeric DNA repeats onto the ends of the chromosomes during cell proliferation. Activation of telomerase is important for the sustained proliferation and development of tumours. Telomerase activity may be useful for cervical cancer screening. hTERT is a catalytic protein subunit of the telomerase enzyme complex and is a rate-limiting component of telomerase activity. These assays may be developed as potential adjuncts for cervical cancer screening.

This study aimed to investigate whether one-stop integrated HPV molecular analysis can facilitate efficient triage of women with equivocal cytology diagnoses, and to enhance understanding of HPV genotypes and transcription in relation to telomerase activity in the development of cervical cancer.

Methods

This study was conducted from January 2008 to December 2009. In a screening population of Hong Kong, HPV DNA (HC2)–positive ASCUS was tested for HPV genotypes, HPV type-specific RNA transcription, and hTERT RNA transcription by SNIPER HPV Genotyping Biochip Assay, nested PCR, and real-time PCR. Correlation between these parameters and outcomes of patients was evaluated.

Among 184 419 liquid-based cervical cytology samples,[1] 7286 (4.0%) were diagnosed with ASCUS. Of 3618 cases undergoing HPV DNA testing using HC2, 1984 (54.8%) were positive for high-risk HPV and 1634 (45.2%) were negative. After checking the RNA quality of the cytology residues of 871 HC2-positive ASCUS, 604 cases were used for HPV

genotyping, HPV type-specific and hTERT RNA transcription. For hTERT study, 20 normal cytology samples, 20 low-grade squamous intraepithelial lesions (LSIL), 15 high-grade SILs (HSIL), and 7 squamous cell carcinomas (SCC) were also included.

The subsequent cytological and colposcopic biopsy findings of patients with ASCUS were retrieved. The findings of LSIL (for cytology) or cervical interstitial neoplasia (for colposcopy) or above were used as cut offs.

DNA and RNA were extracted from the cervical cytology residues of the 871 samples. The quality and quantity were checked. Reverse transcription was carried out on extracted RNA using random hexamer with SuperScript III Reverse Transcriptase (Life Technologies, Carlsbad, CA, USA). HPV genotyping was performed for 604 samples using the locally developed SNIPER HPV Genotyping Biochip Assay.[3] PCR amplification was carried out using biotin-labelled consensus primers targeting for the HPV polymorphic L1 region together with a combination pool of HPV-specific primers designed to amplify 29 HPV genotypes. Primers targeting beta-globin served as a DNA positive control. The biotin-labelled amplicons were hybridised specifically to the immobilised oligonucleotide probes on a membrane-based biochip when the amplicons contained matched sequences of the complementary probes. Following hybridisation, signal visualisation was achieved through colour complex formation with streptavidin peroxidase conjugate. The image of each biochip in the microplate was captured by an imaging system and analysed automatically.

The HPV E6/E7 transcript of various HPV subtypes was evaluated by type-specific nested PCR.[4] Cervical cancer cell lines HeLa, C4-1, SiHa, ME180, and C33A were used as positive and negative controls. The final products amplified from each HPV type-specific nested PCR was separated by gel electrophoresis and visualised by ultraviolet-transillumination after ethidium bromide staining. Both E6 and E7 viral oncogenes of HPV are transcribed from a common promoter. Full length E6/E7 transcript encodes the E6 and E7 proteins, whereas the spliced variants E6*I and E6*II encode truncated E6 proteins with different roles in the virus life cycle in addition to the E7 protein. The size of the amplified products therefore reflected the expression of the full length E6 or truncated E6 proteins. The HPV E6/E7 transcript level was also measured by quantitative PCR (qPCR) using iQ SYBR Green Supermix kits (Bio-Rad Laboratories, Hercules, CA, USA), and inner primers of nested PCR. The relative level was compared with the $\Delta\Delta C_t$ method using the threshold cycle for glyceraldehyde 3-phosphate dehydrogenase (GAPDH) as the normalising control.

The level of hTERT in each sample was compared by qPCR using the relative standard curve method. Both custom-made TaqMan Gene Expression Assay (for Taqman qPCR) targeting exon II of hTERT transcript (Life Technologies, Carlsbad, CA, USA) and primers targeting the same region (for SYBR Green qPCR) were used. The TaqMan assay for GAPDH Hs99999905_m1 was used for normalisation of the amount of cDNA used in each reaction. Full-length cDNA of hTERT and GAPDH were serially diluted and included in each plate for the construction of standard curves.

The Chi-squared test (2-tailed) was used to determine whether the distribution of individual HPV genotype or HPV E6/E7 transcript status differed in cases with different follow-up findings. Mann-Whitney *U* test was used to evaluate the correlation between the level of hTERT transcript and the follow-up findings. Receiver operating characteristic curve analysis was used to determine the cut-off value of the hTERT mRNA level, above which was regarded as 'positive'. Sensitivities, specificities, and positive and negative predictive values of these molecular tests were calculated. A P value of <0.05 was considered statistically significant.

+ve	HPV 16	HPV 18	HPV 31	HPV 33	+ve
HPV 35	HPV 39	HPV 45	HPV 51	HPV 33	HPV 56
HPV 58	HPV 59	HPV 68	HPV 6	HPV 11	HPV 26
HPV 40	HPV 42	HPV 43	HPV 44	HPV 53	HPV 54
HPV 55	HPV 57	HPV 66	HPV 67	HPV 69	HPV 73
	HPV 82	HB	HB	-ve	+ve

HPV 58

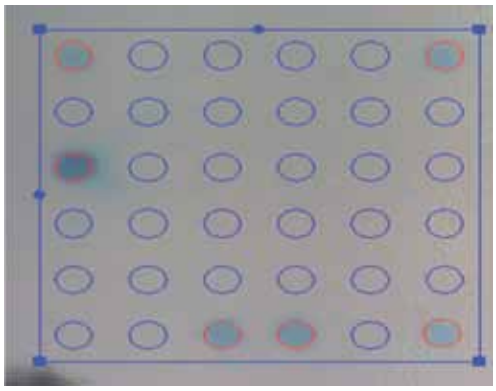

FIG. Human papillomavirus (HPV) genotype HPV58 is identified in a Hybrid Capture 2 test positive sample with atypical squamous cells of undetermined significance using the SNIPER HPV Genotyping Biochip Assay. For control, three spots indicated as positive (+ve) are for colour development control and image alignment. Human beta-globin (HB) serves as an internal control for DNA extraction.

Results

Women with ASCUS who were positive for HPV were more likely to have HSIL (P<0.001, Fisher's exact test) and LSIL or above (P<0.001, Fisher's exact test) detected in follow-up cervical cytology and histology samples.

The HPV genotypes in each ASCUS sample were identified by SNIPER HPV Genotyping Biochip Assay (Fig). The HPV genotype profiles determined by the biochip assay analysis are summarised in Table 1. The five most common high-risk HPV genotypes detected were HPV52 (21.1%), HPV16 (15.5%), HPV58 (15.2%), HPV39 (7.6%), and HPV18 (7.2%). Low-risk HPV genotypes were also detected, but mainly as mixed infection. The six most common types were HPV6 (16.0%), HPV55 (13.8%), HPV44 (12.8%), HPV54 (11.7%), HPV40 (11.7%), and HPV11 (10.6%). This concurred with the focus of HC2 for detection of high-risk HPV. Presence of HPV33 (P=0.001), HPV58 (P=0.024), and HPV68 (P=0.009) correlated with subsequent development of HSIL or above, whereas HPV52 (P=0.025) and HPV31 (P=0.049) correlated with development of LSIL or above. There was no significant difference in outcomes between single or mixed HPV infections.

Full length and spliced variants of E6/E7 transcripts of each HPV genotype could be identified by the size of the amplified products. The distribution of the HPV E6/E7 transcript is summarised in Table 2. To evaluate the significance of HPV oncogenic E6/E7 transcript load, the level of type-specific E6/E7 transcripts was correlated with cytology and biopsy follow-up data. Nested PCR HPV transcription study showed that HPV58 (P=0.023) and HPV59 (P=0.026) mRNA transcripts correlated with subsequent detection of LSIL or above. Correlation between HPV58 mRNA transcripts (P=0.043) and development of HSIL or above was demonstrated by real time PCR.

The hTERT mRNA level significantly increased in each lesion grade (P=0.0129, one-way ANOVA; P=0.0014, test for linear trend). The increase was significant between normal samples and LSIL (P=0.0327), HSIL (P=0.0026), and SCC (P=0.0064), as well as between ASCUS and HSIL (P=0.0401) and SCC (P=0.0319). Among the 600 cases of ASCUS positive for high-risk HPV, the difference was not significant between cases of ASCUS with or without LSIL or above (P=0.696). hTERT/GAPDH level in specific HPV subtype–infected cases was further analysed. In HPV33-infected cases, the hTERT level was significantly higher in cases with a worse follow-up (LSIL or above) [P=0.017]. Among HPV58- (P=0.011), HPV33- (P=0.031), and HPV39- (P=0.045) infected cases, hTERT transcripts correlated with subsequent detection of HSIL or above.

The correlation between E6/E7 mRNA of each HPV genotype and hTERT/GAPDH was conducted using Spearman rho test. Correlation was noted in HPV16- (r=0.486, P<0.000), HPV18- (r=0.557, P<0.000), HPV52- (r=0.704, P<0.000), HPV58- (r=0.451, P=0.003), and HPV33- (r=0.529, P<0.035) infected cases. This indicated that some HPV subtypes may be more capable of inducing oncogenic changes such as telomerase activation.

The sensitivity, specificity, and positive and negative predictive values of HC2 for detecting HSIL or above in this cohort of 3618 cases of ASCUS was 94.3%, 47.6%, 10%, and 99.3%, respectively. Among the HC2-positive ASCUS cases, the specificity and positive predictive value respectively increased to 82.3% and 21.82% after HPV58 genotyping, and to

TABLE 1. Human papillomavirus (HPV) genotypes found in 604 successfully genotyped samples with atypical squamous cells of undetermined significance

HPV genotype	No. (%) of samples with HPV types detected	% of total identifiable HPV genotypes
High risk		
HPV16	112 (15.5)	13.6
HPV18	52 (7.2)	6.3
HPV26	2 (0.3)	0.2
HPV31	23 (3.2)	2.8
HPV33	36 (5.0)	4.4
HPV35	11 (1.5)	1.3
HPV39	55 (7.6)	6.7
HPV45	9 (1.3)	1.1
HPV51	49 (6.8)	5.9
HPV52	152 (21.1)	18.4
HPV53	13 (1.8)	1.6
HPV56	19 (2.6)	2.3
HPV58	110 (15.2)	13.3
HPV59	19 (2.6)	2.3
HPV66	14 (1.9)	1.7
HPV68	38 (5.3)	4.6
82 (MM4)	8 (1.1)	1.0
Subtotal	**722 (100)**	**87.5**
Low risk		
HPV6	15 (16.0)*	1.8
HPV11	10 (10.6)*	1.2
HPV40	11 (11.7)*	1.3
HPV42	6 (6.4)*	0.7
HPV43	9 (9.6)*	1.1
HPV44	12 (12.8)*	1.5
HPV46	1 (1.1)*	0.1
HPV54	11 (11.7)*	1.3
HPV55	13 (13.8)*	1.6
HPV73	6 (6.4)	0.7
Subtotal	**94 (100)**	**11.3**
Indeterminate and other		
HPV67	9 (100)	1.1
Total	**825**	**100**

* Mixed infection

93% and 22.7% after assessment of HPV58 RNA transcript. The corresponding values were 66.0% and 13.4% when hTERT RNA assay alone was used, and 62.8% and 20.0% for hTERT RNA evaluation in HPV58-infected cases.

TABLE 2. Human papillomavirus (HPV) transcripts in cervical cytology samples diagnosed with atypical squamous cells of undetermined significance

HPV genotype (No. evaluated by nested PCR)	No. of samples with either FL or spliced transcript	No. of samples with FL transcript	No. of samples with spliced transcript
HPV16 (n=112)	91/111	90/111	2/111
HPV18 (n=52)	45/52	40/52	5/5
HPV31 (n=23)	21/23	21/23	0/23
HPV33 (n=36)	31/36	31/36	0/36
HPV35 (n=11)	6/11	6/11	1/11
HPV39 (n=55)	37/55	37/55	0/55
HPV45 (n=9)	9/9	9/9	0/9
HPV51 (n=49)	38/49	38/49	0/49
HPV52 (n=152)	141/152	140/152	7/152
HPV58 (n=110)	45/110	40/110	6/110
HPV59 (n=19)	11/19	11/19	0/19
HPV66 (n=14)	12/14	11/14	1/14
HPV68 (n=38)	33/38	33/38	0/38

Discussion

In this study, the five most common high-risk HPV genotypes detected, in decreasing order, were HPV52, HPV16, HPV58, HPV39, and HPV18. These accounted for two-thirds of the HPV genotypes detected. Among ASCUS in this local population, HPV52 and HPV58 were more common than HPV16 and HPV18, with high prevalence in both cervical cancers and precancerous lesions.[5] The distribution of HPV genotypes in different populations varies. This may be due to differences in hospital versus screening populations and the methodology used for HPV genotyping.

About one-quarter of ASCUS in our screening population were HPV negative and did not need colposcopy if HPV vaccine was administered. This may lessen the burden on the screening programme. In addition, HPV33, HPV58, and HPV68 correlated with subsequent detection of HSIL or above, whereas HPV52 correlated with development of LSIL or above. In most studies, HPV16 and/or HPV18 carry prognostic significance. The difference in findings related to disease outcome may be due to the dominant prevalence of HPV58 and HPV52 in this population with ASCUS.

When HPV type–specific RNA transcript status correlated with subsequent follow-up using nested PCR, HPV58 E6/E7 transcription correlated with subsequent development of more serious cervical lesions. Both HPV58 detection and E6/E7 transcription were prominent among the high-risk HPV genotypes.

hTERT transcription levels did not correlate with subsequent detection of serious cervical lesions. Nonetheless, subsequent development of cervical lesions in HPV16- and HPV58-infected cases were noted.

Detection of high-risk HPV by cocktail HC2 achieved a high sensitivity and negative predictive value but moderate specificity and positive predictive value. Additional HPV58 genotyping and RNA transcript assay as well as hTERT assay in HPV58-infected cases enhanced the specificity and positive predictive values. These findings support the use of these adjunct techniques to cytology and HPV DNA testing in triaging women with ASCUS.

Transcription of hTERT correlated with that of HPV16, HPV18, HPV52, HPV58, and HPV33. This suggested significant interaction between HPV and telomerase activity. These HPV genotypes may be more capable of inducing oncogenic changes including telomerase activation. Indeed, HPV oncogenic protein E6 is reported to induce the transcription of hTERT and influence telomerase activity leading to cell immortalisation and cervical carcinogenesis.

Acknowledgements

This study was supported by the Research Fund for the Control of Infectious Diseases, Food and Health Bureau, Hong Kong SAR Government (#07060562). The high-risk HPV Hybrid Capture 2 test was supported by the SK Yee Medical Foundation. The authors thank Dr Kar-Fai Tam for help in collecting clinical samples and Dr Stephanie Liu for collecting the cervical cancer cell lines HeLa, C4-1, SiHa, ME180, and C33A, and Prof Paul Chan for the reference on SNIPER HPV Genotyping Biochip Assay. We also thank Miss Lily Fung and Miss Candy Lau for their secretarial and clerical support, and all colleagues, doctors, technical staff, patients, and participants who contributed to this project.

References

1. Cheung AN, Szeto EF, Ng KM, et al. Atypical squamous cells of undetermined significance on cervical smears: follow-up study of an Asian screening population. Cancer 2004;102:74-80.
2. Cheung AN. Molecular targets in gynaecological cancers. Pathology 2007;39:26-45.
3. Yip YC, Ngai KL, Vong HT, et al. Prevalence and genotype distribution of cervical human papillomavirus infection in Macao. J Med Virol 2010;82:1724-9.
4. Molden T, Nygard JF, Kraus I, et al. Predicting CIN2+ when detecting HPV mRNA and DNA by PreTect HPV-proofer and consensus PCR: A 2-year follow-up of women with ASCUS or LSIL Pap smear. Int J Cancer 2005;114:973-6.
5. Chan PK, Li WH, Chan MY, Ma WL, Cheung JL, Cheng AF. High prevalence of human papillomavirus type 58 in Chinese women with cervical cancer and precancerous lesions. J Med Virol 1999;59:232-8.

Published by the Hong Kong Academy of Medicine Press for the Government of the Hong Kong Special Administrative Region. The opinions expressed in the *Hong Kong Medical Journal* and its supplements are those of the authors and do not reflect the official policies of the Hong Kong Academy of Medicine, the Hong Kong Medical Association, the institutions to which the authors are affiliated, or those of the publisher.